Bio-inspired adaptive control strategy for the highly efficient speed regulation of the DC motor under parametric uncertainty

Alejandro Rodríguez-Molina[a], Miguel G. Villarreal-Cervantes[a,*], Jaime Álvarez-Gallegos[b], Mario Aldape-Pérez[a]

[a]*Posgraduate Department, Instituto Politécnico Nacional - CIDETEC, Mexico city, 07700, Mexico.*
[b]*Electric Engineering Department, Instituto Politécnico Nacional - CINVESTAV, Mexico city, 07360, Mexico.*

Abstract

The presence of parametric uncertainties decreases the performance in controlling dynamic systems such as the DC motor. In this work, an adaptive control strategy is proposed to deal with parametric uncertainties in the speed regulation task of the DC motor. This adaptive strategy is based on a bio-inspired optimization approach, where an optimization problem is stated and solved online by using a modification of the differential evolution optimizer. This modification includes a mechanism that promotes the exploration in the early generations and takes advantage of the exploitation power of the DE/best class in the last generations of the algorithm to find suitable optimal control parameters to control the DC motor speed efficiently. Comparative statistical analysis with other bio-inspired adaptive strategies and with linear, adaptive and robust controllers shows the effectiveness of the proposed bio-inspired adaptive control approach both in simulation and

*Corresponding author: E-mail address: mvillarrealc@ipn.mx

experimentation.

Keywords: Bio-inspired adaptive control, bio-inspired techniques, control parameter estimation, differential evolution, optimization problem.

Acronyms

ACS Adaptive Control Strategy

DE Differential Evolution

GA Genetic Algorithm

GPIRC Generalized Proportional Integral Observer based Robust Controller

IAE Integral Absolute Error

IDE Improved Differential Evolution

ISE Integral Squared Error

ITAE Integral Time-weighted Absolute Error

MRAC Model Reference Adaptive Controller

PI Proportional Integral

PID Proportional Integral Derivative

PSO Particle Swarm Optimization

1. Introduction

DC motors are used in a wide variety of applications. This fact is associated with their relatively low cost, high durability, and easy controllability by varying its input. In industry, they are commonly used as the main actuation devices in robotic arms [1], vehicles [2], machine tools [3] and others. In most of those applications, high accuracy rates are required for the motor tasks of tracking and regulation. In order to achieve this requirement, control systems aim to provide the best/desired motor dynamic behavior to perform a determined action.

Along time, there have been proposed many control systems that afford the best performance of motors under different conditions. For example, linear controllers are a kind of control systems that establish a linear relationship between the desired and current states of the motor. Linear controllers are extensively used in industry because of their simplicity and good performance [4]; nevertheless, all real-world systems are no-linear, and a linear control approach could not be enough to achieve the best performance, because the plant dynamics are highly nonlinear or there are always uncertainties. On the other hand, nonlinear controllers can improve the stability of dynamic systems, but they usually have more complex structures such that the practical implementation is more challenging than that of linear controllers [5]. Among the nonlinear controllers are those that use the model of the system dynamics (model-based control systems) which have high performance as long as the physical parameters of the plant are well-known. However, when there are significant differences between the known parameters and the real ones, the model-based control systems may perform improperly [6]. Even if those controllers fulfill this feature, their operation performance may be affected by the presence of parametric uncertainties or unmodeled dynamics.

Parametric uncertainties are undesirable and in many cases unpredictable behaviors of the plant parameters. They are responsible for low control performance and consequently for the deficient operation of the plant [7]. These uncertainties may arise due to the plant wear after the continuous and unstopped operation, and the operation environment properties, such as temperature and viscosity, among others.

Adaptive control, robust control, and optimal controller tuning approaches have been used to deal with parametric uncertainties.

The robust control approach [8] can deal with a set of bounded uncertainties. In robust control, the uncertainties are considered as unknown mismatches of the dynamic model, and then, the robust controller is designed based on this imperfect model [8]. Robust control aims to maximize the uncertainties and at the same time preserve the desired controller performance [9], i.e., the controller sensitivity to the difference between the imperfect model and the real system is minimized. Robust control has been widely studied, and several algorithms have been developed for high-performance speed regulation of the DC motor [10–13]; nevertheless, the assumption of bounded uncertainties behavior can carry some issues when the real system is highly disturbed.

The optimal controller tuning approach is related to the adjustment of the control system parameters based on an optimization process. There are some recent works under this approach in which it has been possible to obtain the best control parameters that improve the operation of dynamic systems under different conditions and for diverse tasks. In order to achieve this, a formal optimization problem is stated and solved off-line by using an optimizer. The solution to this problem contains the best control parameters, which are implanted in the control system and remain fixed [14–16]. In [17] for example, the gains of a Proportional Integral (PI) controller for the speed control of a photovoltaic fed DC motor, are optimally tuned off-line by the Bacteria Foraging Optimization Algorithm (BFOA) and the Firefly Algorithm (FA), respectively. In this case, the speed control is achieved with promising performance and robustness to load changes. On the other hand, a similar tuning methodology is successfully applied to the PI controllers of the photovoltaic fed Switched Reluctance Motor (SRM) in [18] and of the wind turbine fed Induction Motor (IM) in [19], by using the Ant Colony Optimization (ACO) and the Imperialist Competitive Algorithm (ICA), respectively. A comparative study between the Genetic Algorithm (GA) and the Particle Swarm Optimization (PSO) meta-heuristics in the PI off-line controller tuning for a quadruple-tank process is presented in [20]. In that work, the PSO based PI controller has the most promising performance. A similar study is provided in [21] where the GA, PSO, an Evolutionary Programming (EP) technique and the ACO are used in the Proportional Integral Derivative (PID) controller off-line tuning. This time the GA based controller achieves the best performance. In both cases, some comparisons with controllers obtained with classical tuning approaches are included, obtaining an outstanding performance with the meta-heuristic based alternatives. Despite the proved effectiveness of the above control systems, the main drawback is the necessity of knowing the states of the system during an execution time window and the information about the behavior of uncertainties, which in almost all cases is very hard to satisfy.

On the other hand, adaptive control is a term used to refer to a class of control strategies that estimate the control parameters online by using the system feedback (they can be the control gains or the physical parameters of the plant). The obtained parameters are used in calculating an adequate control signal that stabilizes the plant behavior and compensates the uncertainties [22].

Adaptive control has been studied from different approaches. Many adaptive control strategies have been designed based on Lyapunov stability or by using a sensitivity index of the system output in the presence of disturbances [23–25]. The aim is the convergence of the estimated parameters to the real ones after a certain period. Nevertheless, these strategies have some issues when there are high-frequency parametric uncertainties [26], i.e., there is a trade-off between the convergence speed of the estimated parameters and the stabilization of the closed-loop system.

A relatively recent approach to adapt the control parameters online is based on the use of artificial intelligence techniques. Among the most commonly used techniques are neural networks and fuzzy logic. Adaptive control systems based on neural networks [27–29] include weighted networks fed by the dynamic system inputs which produce an output that contains a suitable set of control parameters based on weighting and interconnection operations. On the other hand, adaptive control systems based on fuzzy logic use fuzzy rules (*if-then* rules) to online estimate the control parameters. These rules require a fuzzy set based on the dynamic system input and output information, which is transformed by a defuzzification method to select the most appropriate control parameters [30, 31]. Many of these works include an optimization process to obtain the best intelligent controller configurations (commonly, the parameters of the neural networks or fuzzy systems) that handle particular dynamic system behaviors and operation conditions.

Moreover, this kind of intelligent controllers has been successfully applied to control DC motors. In [32], the optimal parameters of an Adaptive Neuro-Fuzzy Inference System Controller are tuned through an optimization approach based on the Bat Algorithm. On the other hand, in [33], a Fuzzy PID Supervised Online Recurrent Fuzzy Neural Network Based Controller is tuned with the aid of the Anlion optimizer. In both of the above works, the tuned controllers are used in the speed controls of DC motors and fit desired performance level under several well-defined operating conditions. As it can be noticed, the intelligent adaptive control approach can achieve high performance in the stabilization of the closed-loop system with the presence of specific parametric uncertainties. Nonetheless, these require *a priori* knowledge of the input and output signals of the dynamic system subject to specific disturbances to be off-line trained or adjusted. The above becomes a problem since uncertainties are often unpredictable.

Unlike the approaches presented at this point, an online optimization approach to adaptive control can provide a suitable parameter adaptation at each time instant. It means that for each sampling time instant, a different set of optimal control parameters is obtained by an optimizer as a solution of a dynamic optimization problem. Nevertheless, the optimizer remarkably influences in the performance of the adaptive control. Deterministic optimizers require information about the problem to be solved such as the gradient vector to guide the search for the best solution into the neighborhood of a proposed initial solution [34–36]. When parametric uncertainties exist, the best solution dynamically changes its position in the search space, and this may affect the search capability of the deterministic optimizers due to the high sensitivity of their requirements mentioned above. In that case, the stochastic optimizers such as the bio-inspired ones can deal with those difficulties [37].

Nevertheless, the bio-inspired adaptive control approaches (those in which an online optimization problem is stated and solved by using a bio-inspired optimizer) have been studied a little. In [38], the gains of an integral and proportional (IP) controller of a Linear Induction Motor (LIM) are online obtained by stating an optimization problem and solving it by using the GA. Despite the satisfactory results obtained in that work, there is not enough statistical evidence to guarantee the appropriate operation of its control strategy.

When stochastic techniques are selected as optimizers, full statistical evidence must be presented to conclude that results will be reliable in future runs [39]. In [40], the performance of several meta-heuristic optimizers in the adaptive control of the DC motor is compared in simulation by using descriptive and non-parametric statistical analysis. Unlike those results, this work has been substantially modified regarding algorithmic features, problem statement and experimental analysis, in order to statistically show the feasibility of the proposed bio-inspired adaptive control approach in a real prototype and determine its advantages based on experimental comparative performance analysis with advanced and recent controllers. Then, in the present work, the bio-inspired adaptive control strategy is based on a novel improved variant of the Differential Evolution (DE) optimizer and is used to find the optimal control parameters of a DC motor online. This variant includes a diversity mechanism aiming to perform an efficient explorative search into an uncertain dynamic environment [41] and to avoid the premature convergence of the algorithm, which implies to regulate the DC motor speed under parametric uncertainties efficiently.

On the other hand, changes in the constrained dynamic optimization problem are done to perform the experimental tests. In the new problem, three parameters must be dynamically found through the time evolution which increases the multi-modality of the problem because more solutions satisfy the performance criterion. Hence, the main contribution of this work is the proposal of a bio-inspired adaptive control strategy based on an improvement of the DE algorithm for the highly efficient speed regulation of the DC motor and its fair comparative performance analysis with other classical and advanced controllers with experimental evidence. Moreover, the theoretical validation of this approach is given by the control theory.

The paper is organized as follows: In Section 2, the bio-inspired adaptive control strategy based on an online constrained dynamic optimization problem is stated and the Improved Differential Evolution (IDE) optimizer is also described. A stability test of the proposed control strategy is performed in Section 3. Section 4 includes the analysis of the simulation and experimental results. Finally, in Section 5 conclusions are drawn, and future work is presented.

2. Proposed bio-inspired adaptive control strategy

The general operation of the proposed bio-inspired adaptive control strategy is shown in Fig. 1. This strategy aims to reduce the error in the speed regulation task of the DC motor. For that, an optimization problem is stated and solved online. A solution of the problem $\bar{\theta}^*$ (where $\bar{\theta}^*$ denotes the best of a set of different $\bar{\theta}$ solutions) must contain the control parameters that minimize the error between the current states z (acquired from the real DC motor) and the estimated states $\bar{z}$ (obtained from an estimated dynamic model). The solution $\bar{\theta}^*$ is obtained with the aid of the proposed bio-inspired optimizer and is used in calculating the control signal for each sampling instant $\triangle t$.

It is important to highlight that z includes the angular speed and acceleration of the motor, but these values are experimentally estimated by using the symmetric difference quotient and the Kalman filter, respectively, which are explained in detail in the later sections.

2.1. Constrained dynamic optimization problem

The objective functions in (1) and (2) are included into the constrained dynamic optimization problem (CDOP) to dynamically find an optimal vector $\bar{\theta}^* = [\bar{\theta}_0^*, \bar{\theta}_1^*, \bar{\theta}_2^*]^T$ for each sampling time $\triangle t$. Those functions (J_1 and J_2) consider the integral squared error among the current states z and the estimated ones $\bar{z}$ for a time interval $\Omega \in [t_{opt} - \triangle w, t_{opt}]$, where t_{opt} is the time instant when the optimization process is performed and $\triangle w$ is the time interval in which the past states z of the motor and of the estimated states $\bar{z}$ are used in the error calculation. It is worth to mention that before the first $\triangle w$ instant, there is no enough information about the motor states, then the

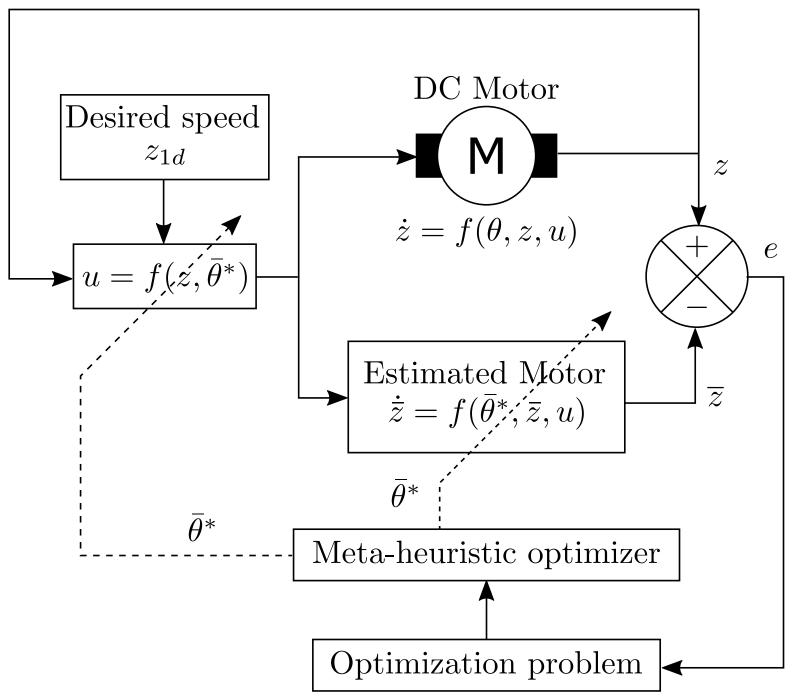

Figure 1: Proposed control strategy.

parameters $\bar{\theta}^*$ cannot be obtained and is necessary to use a constant control signal u_0 until reaching $\triangle w$.

$$J_1 = \int_{t\in\Omega} \left(z_1\left(\theta, t\right) - \bar{z}_1\left(\bar{\theta}, t\right)\right)^2 dt \tag{1}$$

$$J_2 = \int_{t\in\Omega} \left(z_2\left(\theta, t\right) - \bar{z}_2\left(\bar{\theta}, t\right)\right)^2 dt \tag{2}$$

Solving a multi-objective optimization problem is always more expensive in computational time than solving a single-objective one. Taking into account that the proposed adaptive control strategy must solve the optimization problem online (at each sampling time $\triangle t$), the weighted sum method [42] is used to transform this problem into a single objective one as $J = J_1 + J_2$.

2.1.1. Constraints

For simulation results, it is necessary to model the behavior of the DC motor. Then, one of the dynamic constraints is related to the dynamic model of the DC motor. The dynamic model of the DC motor is given in (3) and (4) and its electro-mechanic diagram is shown in Fig. 2, where q, $\dot{q}$, $\ddot{q}$ are the angle, the angular speed and the angular acceleration of the shaft, i_a is the armature current, J_0 is the rotor moment of inertia, k_m is the torque constant, b_0 is the viscous friction constant, τ_L is the load torque, R_a is the armature resistance, L_a is the armature inductance, k_e is the electromotive force constant and V is the input voltage.

$$L_a \frac{di_a}{dt} + R_a i_a + k_e \dot{q} = u \tag{3}$$

$$J_0\ddot{q} + b_0\dot{q} = k_m\left(i_a - \frac{\tau_L}{k_m}\right) \tag{4}$$

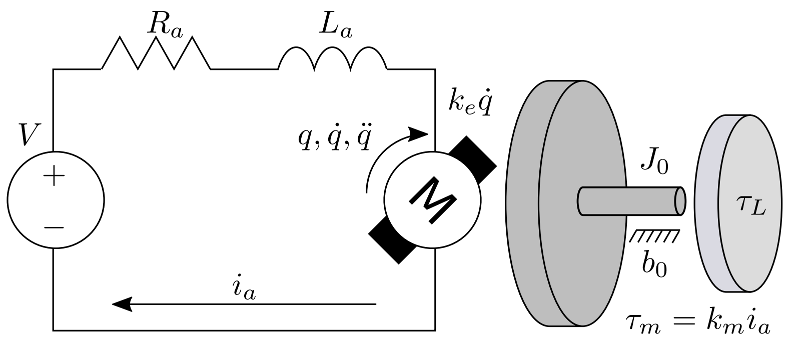

Figure 2: Electro-mechanic diagram of the DC Motor.

Unlike the optimization problem given in [40], in this paper the DC motor dynamic model is transformed into the state space $z = [z_1, z_2]^T = [\dot{q}, \ddot{q}]^T$, then the dynamic model in (3) and (4) can be written as in (5) assuming $\tau_L = 0$, where $\theta_0 = k_e + \frac{R_a b_0}{k_m}$, $\theta_1 = \frac{J_0 R_a}{k_m} + \frac{L_a b_0}{k_m}$ and $\theta_2 = \frac{J_0 L_a}{k_m}$.

$$\dot{z}_2 = \frac{1}{\theta_2}u - \frac{\theta_0}{\theta_2}z_1 - \frac{\theta_1}{\theta_2}z_2 \tag{5}$$

This coordinate change is required for experimental purposes in order to reduce the sensor devices.

Hence, dynamic constraints are related to the DC motor dynamics $\dot{z} = f(\bar{\theta}, z, u)$ and to the load free estimated DC motor dynamics given in (6) for all $t \in \Omega$ considering the initial conditions $z = [0, 0]^T$ and $\bar{z}(t_{opt} - \triangle w) = z(t_{opt} - \triangle w)$, respectively. For experimental results (laboratory testing with a real prototype), the constraint related to the DC motor dynamics is removed because the current states are given through the use of angular position sensors and/or through an estimation.

$$\dot{\tilde{z}}_2 = \frac{1}{\bar{\theta}_2}u - \frac{\bar{\theta}_0}{\bar{\theta}_2}\bar{z}_1 - \frac{\bar{\theta}_1}{\bar{\theta}_2}\bar{z}_2 \tag{6}$$

The controller u in (7) is proposed for the speed regulation of the DC motor, where $v = K_p^{acs}\tilde{z}_1 + K_d^{acs}\tilde{z}_2$, $\tilde{z}_1 = z_{1d} - z_1$ and $\tilde{z}_2 = z_{2d} - z_2 = -z_2$ with K_p^{acs} and K_d^{acs} as the proportional and derivative gains, z_{1d} and z_{2d} as the desired speed and acceleration.

$$u = \bar{\theta}_2 v + \bar{\theta}_0 z_1 + \bar{\theta}_1 z_2 \tag{7}$$

Additionally, the maximum and minimum bounds of the control signal (8) given by the capacity of the power source are set as constraints.

$$u_{min} \leq u(t_{opt}) \leq u_{max} \tag{8}$$

2.2. Bio-inspired optimizer

Usually, the real-world optimization problems are tough to solve. Nevertheless, bio-inspired optimizers can get useful solutions to these problems with a reasonable computational cost. Moreover, they do not require special conditions such as continuity or differentiability of the optimization problem [43]. That is why they are increasingly being used in recent years.

Despite the advantages of bio-inspired optimizers, the *No Free Lunch Theorem* establishes that there is no universal bio-inspired optimizer capable of solving all kinds of problems [44]. For this reason, it is necessary to identify the problem nature and choose the fittest bio-inspired optimizer. This process may include the testing of different optimizers and performing changes in their search mechanisms.

Differential Evolution (DE) is an optimizer bio-inspired in the process of natural evolution [45] since it includes Neo-Darwinism theory evolutionary operators like mutation, crossover, and selection. It is well-known and widely used because of its simplicity, high effectiveness and applicability in solving real-world problems [46–48]. The general operation of DE is shown in Algorithm 1. In this optimizer, an initial population of $X_0 \in R^{NP \times D}$ individuals (NP design vectors of dimension D) is generated randomly in the search space. For each generation G (from the first generation until G_{max}), the NP individuals in population $X_G \in R^{NP \times D}$ called parents are mutated and recombined to create new offspring individuals. For every new generation, the greedy selection is made between the parents and offsprings according to their fitness (the value of the objective function). Finally, the best individuals are found in the last generation of the population.

Remarking for this particular problem, the population X_G contains NP different solution vectors $\bar{\theta}$ and at the end of the algorithm, the vector $\bar{\theta}^*$ is selected from $X_{G_{max}}$ according to the fitness value J.

Algorithm 1 Differential Evolution

Generate initial population X_0 with NP individuals
Evaluate X_0
$G \leftarrow 0$
while $G \leq G_{max}$ **do**
  for each $x_i \in X_G$ **do**
    Generate a mutant individual v_i
    Generate an offspring individual u_i
    Evaluate u_i
  end for
  Select individuals for G+1
  $G \leftarrow G + 1$
end while
$\bar{\theta}^* = x_{best}$

Different DE variants have been proposed [45] and each one aims to improve the exploration (the process to identify potentially good regions of the search space) and exploitation (the process to refine an identified region) capabilities of DE [49]. The differences among the DE variants lie in the different ways to perform the mutation and recombination operations, and in the number of parents used to generate a new individual. These variants follow a simple nomenclature $DE/a/b/c$, where "a" refers to the base individual used to generate a mutant, "b" is the number of difference vectors (a vector generated by the difference of two different parents randomly selected from population), and "c" is the recombination operation used to generate the offspring by combining a parent individual with the generated mutant

[50].

This paper compares a proposed improved DE (IDE) with the performance of variants which include *Best* individuals in the evolutionary process and involve discrete recombination, arithmetic recombination and a combined discrete - arithmetic recombination.

2.2.1. Discrete recombination with best individuals

Discrete recombination includes binomial and exponential crossover [51]. In binomial crossover each part of the coded information ($j-th$ design variable) of the $i-th$ offspring $u_{i,j}$ has the same crossover probability (CR) in the interval $[0,1]$ to include information from the parent $x_{i,j}$ or the mutant vector $v_{i,j} = x_{best,j} + F(x_{r_1,j} - x_{r_2,j})$ with x_{r_1} and x_{r_2} two randomly selected individuals and x_{best} the best individual in population. On the contrary, with exponential crossover, the information of the parent is consecutively passed to the offspring until a random number surpasses the crossover probability CR. At that moment, the remaining information is passed from the mutant vector. The scale factor (F) provides the mutation rates and it is in the interval $[0,1]$. The pseudo-code of the discrete recombination is shown in Algorithms 2 and 3. The variants of DE that use discrete recombination with best individuals are referred as DE/best/1/bin and DE/best/1/exp for the binomial and exponential crossover, respectively.

Algorithm 2 Binomial crossover

function BINOMIALCROSSOVER(x_i,v_i)
    $u_i \leftarrow x_i$
    $k \leftarrow irandom(1, D)$
    for $j \leftarrow 1$ **to** D **do**
        if $random(0, 1) < CR$ **or** $j = k$ **then**
            $u_{i,j} \leftarrow v_{i,j}$
        end if
    end for
    return u_i
end function

Algorithm 3 Exponential crossover

function EXPONENTIALCROSSOVER(x_i,v_i)
    $u_i \leftarrow x_i$
    $k \leftarrow irandom(1, D)$
    $j \leftarrow k$
    $L \leftarrow 0$
    do
        $u_{i,j} \leftarrow v_{i,j}$
        $j \leftarrow mod(j, D) + 1$
        $L \leftarrow L + 1$
    while $random(0, 1) < CR$ **&** $L \neq D$
    return u_i
end function

2.2.2. *Arithmetic recombination with best individuals*

Arithmetic recombination is different from the discrete crossover operation since this is rotation invariant. The offspring $u_i = v_i$ is generated by linearly perturbing x_i by using recombination differentials and mutation differentials. In this case, the arithmetic recombination in (9) is used. The recombination differentials are those difference vectors where the base vector appears in them. In (9), the recombination differential is the difference vector between x_i and the best individual x_{best} among the population. The mutation differentials are those vectors that do not include the base vector. In (9), the mutation differential is the difference vector between two different random individuals (x_{r_1} and x_{r_2}). The parameter K is the crossover rate in the interval $[0, 1]$ to provide linear recombination. The DE variant that uses arithmetic recombination with the best individual is referred to as DE/current-to-best/1.

$$v_i = x_i + K(x_{best} - x_i) + F(x_{r_1} - x_{r_2}) \tag{9}$$

2.2.3. *Combined discrete - arithmetic recombination with best individuals*

In the combined discrete - arithmetic recombination the vector v_i in the arithmetic recombination (9) is included into the binomial (see Algorithm 2) or exponential (see Algorithm 3) discrete recombinations. The DE variants that use the combined discrete-arithmetic recombination with the best individual are referred as DE/current-to-best/1/bin and DE/current-to-best/1/exp.

2.2.4. Proposed improvement

The IDE algorithm is proposed to be used with the adaptive control strategy. Algorithm 4 shows the operation of the improved DE. As it can be seen, this version is similar to the DE/best/1/bin variant of DE where the best individual of each generation is used to generate a mutant. The main two differences with IDE lie in the binomial crossover and the selection process. In the binomial crossover, only the $j-th$ randomly selected design parameter $v_{i,j}$ is included into the $j-th$ design variable of the offspring $u_{i,j}$. Otherwise, the information of the parent vector is included. The above is the same as set the crossover rate as $CR = 0$ in the Algorithm 2. In the selection process for the generations before $PC \times G_{max}$, where PC is a percentage of all generations in the interval $[0, 1]$, the best individual is not selected as the best of the entire population but is selected by tournament in order to prevent the premature convergence of the optimizer to a local minimum. In the tournament selection operation described in Algorithm 5, the best individual is obtained from a competition among TS randomly selected contestants, then this elite individual cannot be only the best of the whole population but the best of a reduced group [52]. After the $PC \times G_{max}$ generations, the criterion to select the best individual turn out to be the same as in DE/best/1/bin to enhance the exploitation by the end of the optimization process. It is important to mention that the DE/best/1/bin variant of DE is selected to be used by IDE because it includes some advantageous features of the DE/best class. This particular class of DE variants provides a faster convergence to promising solutions [53]. For the proposed control strategy, this is a desirable feature since the solution of the optimization problem must be obtained in a short time (less than the sampling time $\triangle t$).

Algorithm 4 Improved Differential Evolution

Generate initial population X_0 with NP individuals
Evaluate X_0
$G \leftarrow 0$
while $G \leq G_{max}$ **do**
    if $G \leq PC \times G_{max}$ **then**
        Select the best individual by tournament x_{best}
    else
        Select x_{best} as the best individual in population
    end if
    for each $x_i \in X_G$ **do**
        Generate a mutant individual v_i
        Generate an offspring individual u_i
        Evaluate u_i
    end for
    Select individuals for G+1
    $G \leftarrow G + 1$
end while
$\bar{\theta}^* = x_{best}$

Algorithm 5 Selection by tournament

function SELECTION()
    $rand \leftarrow irandom(1, NP)$
    $x_{best} \leftarrow x_{rand}$
    $t \leftarrow 0$
    while $t < TS$ **do**
        $rand \leftarrow irandom(1, NP)$
        if $f(x_{rand}) < f(x_{best})$ **then**
            $x_{best} \leftarrow x_{rand}$
        end if
        $t \leftarrow t + 1$
    end while
    return x_{best}
end function

2.2.5. Constraint handling

For solving the constrained optimization problem stated before, a mechanism to handle constraints is implemented to work along with the DE variants. This mechanism is known as the criterion of Deb and is used to decide whether one solution is better than another [54]. The criterion of Deb states the following:

- Any feasible is preferred to an infeasible solution.
- Among two feasible solutions, the one having better objective function value is preferred.

- Among two infeasible solutions, the one having smaller constraint violation is preferred.

Additionally to the criterion of Deb, if two infeasible solutions have the same constraint violation, the preferred solution is chosen randomly.

3. Stability test

Let assume that a suitable solution of the dynamic optimization problem given in Subsection 2.1 is found, then the controller in (7) asymptotically stabilizes the dynamic system (5) at the origin $[\tilde{z}_1, z_2]^T = [0, 0]^T$.

Proof. Let the change of coordinates $[\tilde{z}_1, z_2]^T$ where $\tilde{z}_1 = z_{1d} - z_1$, then the candidate Lyapunov function in (10) is considered.

$$V(\tilde{z}_1, z_2) = \frac{1}{2}\bar{\theta}_2 z_2^2 + \frac{1}{2}\bar{\theta}_2 K_p^{acs} \tilde{z}_1^2 \tag{10}$$

The derivative with respect to time of (10) is given in (11).

$$\dot{V} = \bar{\theta}_2 z_2 \dot{z}_2 + \bar{\theta}_2 K_p^{acs} \tilde{z}_1 \dot{\tilde{z}}_1 \tag{11}$$

Assuming that the performance of the bio-inspired optimizer provides a solution ($\bar{\theta}^*$) of the problem in Subsection 2.1 which implies that $J = J_1 + J_2 = 0$ and consequently $J_1 = 0$ and $J_2 = 0$ (since $J_1, J_2 \in R^+$), then the error between the current states z and the estimated ones $\bar{z}$ must be decreased to zero and hence $\bar{z} = z$. Therefore, the estimated DC motor dynamics in (6) can be written as in (12).

$$\dot{z}_2 \bar{\theta}_2 = u - \bar{\theta}_0 z_1 - \bar{\theta}_1 z_2 \tag{12}$$

Substituting u from (7) in (12), the obtained closed-loop system is expressed in (13).

$$\dot{z}_2 = K_p^{acs}\tilde{z}_1 - K_d^{acs}z_2 \tag{13}$$

Using (13) in (11) results:

$$\dot{V} = -\bar{\theta}_2 K_d^{acs} z_2^2 \leq 0 \tag{14}$$

Based on the La Salle's invariance principle, $\dot{V} = 0 \Longrightarrow [\tilde{z}_1, z_2]^T = [0, 0]^T$, the origin $[z_2, \tilde{z}_1]^T = [0, 0]^T$ is asymptotically stable.

□

4. Results

4.1. Simulation details

For simulation purposes, the DC motor speed must be regulated to $z_{1d} = 52.35\ rad/s = 500\ rpm$ during $15s$. The sampling time is set to $\triangle t = 5\ ms$. Parametric uncertainties are included into the DC motor dynamics. The disturbances given in Table I are added to the nominal motor parameters. As it can be seen in Table I, the parameters R_a, L_a, k_m and k_e are continuously disturbed during the execution time $t \in [0, 15]s$ and they sinusoidally vary up to 10% of their nominal values. Additionally, two discontinuous disturbances are included. In the first one, the nominal values of b_0 and J_0 are increased to 300% and 930% from their nominal values, respectively in the time interval $t \in [10, 13]$. In the second one, a disturbance ξ is added to (5) when $t \in [4, 7]s$.

Table I: Results dynamic.

Nominal value	Disturbed value
$R_a = 9.665\ \Omega$	$R_a(t) = R_a + 0.1R_a sin\left(\frac{2\pi}{3}t\right)$
$L_a = 102.44 \times 10^{-3}\ H$	$L_a(t) = L_a + 0.1L_a sin(\pi t)$
$k_m = 0.3946\ N \cdot m/A$	$k_m(t) = k_m + 0.1k_m sin\,(2\pi t)$
$k_e = 0.4133\ V \cdot s/rad$	$k_e(t) = k_e + 0.1k_e sin\,(2\pi t)$
$b_0 = 5.85 \times 10^{-4}\ N \cdot m \cdot s$	$b_0(t) = b_0 + 17.55 \times 10^{-4}\ N \cdot m \cdot s$ **when** $t \in [10, 13]s$
$J_0 = 3.45 \times 10^{-4}\ N \cdot m \cdot s^2$	$J_0(t) = J_0 + 32.1648 \times 10^{-4}\ N \cdot m \cdot s^2$ **when** $t \in [10, 13]s$
$\xi = 0$	$\xi = -0.05\frac{R_a}{J_0 L_a}$ **when** $t \in [4, 7]s$

In terms of θ_0, θ_1 and θ_2, the DC motor parameters vary up to 20%, 1100% and 1100% respectively. Fig. 3 shows the nonlinear behavior of the parameters θ_0, θ_1, θ_2 and the disturbance ξ.

The previously described conditions are used to test the performance of the proposed bio-inspired control strategy named as Adaptive Control Strategy (ACS) based on the IDE (ACS-IDE). The strategy parameters are set as $\triangle w = 50\ ms$, $u_{min} = -48\ V$, $u_{max} = 48\ V$, $u_0 = 20\ V$. The controller in the proposed strategy has the gains $K_p^{acs} = 6700$ and $K_d^{acs} = 350$.

In the present work, seven bio-inspired adaptive control strategies based on different DE variants are selected to perform the test and make comparisons. These strategies are based on five different DE variants and two optimizers recurrently used in many controller tuning applications (GA and PSO) [55–57]. The adopted strategies are listed below:

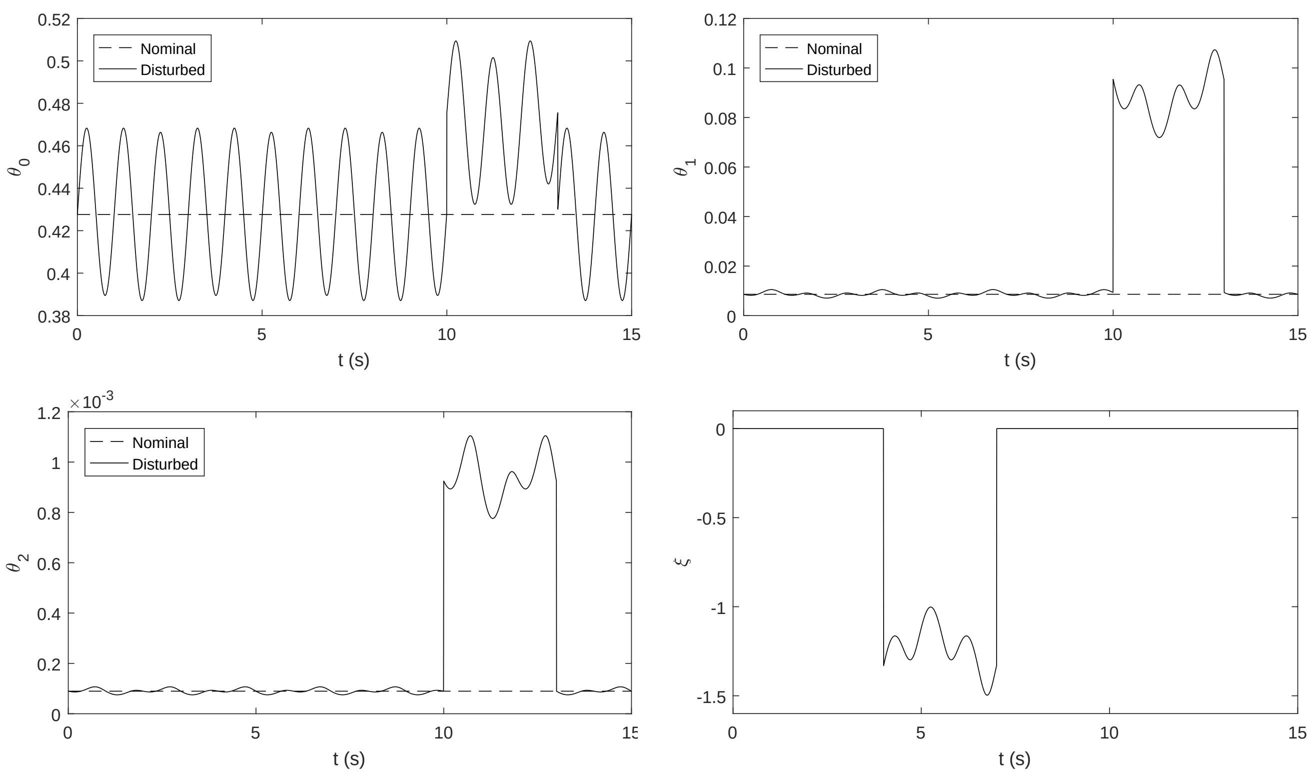

Figure 3: Behavior of the DC motor parameters in terms of θ_0, θ_1, θ_2 and the disturbance ξ.

- Bio-inspired adaptive control alternatives:
  - ACS-DE/best/1/bin
  - ACS-DE/best/1/exp
  - ACS-DE/current-to-best/1
  - ACS-DE/current-to-best/1/bin
  - ACS-DE/current-to-best/1/exp
  - ACS-GA
  - ACS-PSO

It is important to highlight that the parameters of any bio-inspired optimizer in these adaptive control strategies have a crucial role in their effectiveness in finding appropriate solutions [58]. So, for two different parameter configurations of the same optimizer, different performances may be achieved. In order to perform fair comparisons among the optimizers in the proposed adaptive control strategy, all of them are tuned iteratively by using the package *i-race* of the statistical software *R*.

The tuned parameters of the DE variants are shown in Table II. In this, the parameters K and F are randomly obtained in the intervals $[K_{min}, K_{max}]$ and $[F_{min}, F_{max}]$, respectively for each generation, while CR is a fixed parameter.

The selected GA uses the SBX [59] and PM [60] real-coded genetic operators with distribution indexes η_c and η_m, and probabilities pc and pm, respectively. Moreover, an elitist selection is adopted to retain only the fittest NP individuals for each generation. The tuned GA parameters are shown in Table III.

Table II: Parameters of the DE variants.

Variant	CR	F_{min}	F_{max}	K_{min}	K_{max}	PC	TS
DE/best/1/bin	0.472	0.568	0.729	-	-	-	-
DE/best/1/exp	0.630	0.942	0.950	-	-	-	-
DE/current-to-best/1	-	0.618	0.869	0.813	0.959	-	-
DE/current-to-best/1/bin	0.494	0.706	0.873	0.485	0.570	-	-
DE/current-to-best/1/exp	0.345	0.540	0.676	0.176	0.764	-	-
IDE	0.000	0.699	0.768	-	-	0.317	17

The adopted PSO variant is described in [61] and includes a linear decreasing inertia weight [62]. The tuned PSO parameters are shown in Table III where C_1 and C_2 are the weights that ponder the swarm and the personal knowledge, and V_{min}, V_{max} are the bounds of the inertia factor.

For all optimizers, the population size is set as $NP = 25$ and the stop condition uses a maximum number of generations of $G_{max} = 60$, then 1500 evaluations of the objective function J are performed for each optimization process. The search space of the dynamic optimization problem is bounded according to Table IV. These bounds are selected taking into account the magnitude of the nominal values of the DC motor parameters, considering a reasonably large threshold for the search.

In addition to the bio-inspired adaptive control alternatives; linear, adaptive and robust controllers are considered to make comparisons. Those controllers are named and grouped in this paper as classical-advanced control strategies and are the following:

- Classical-advanced control strategies:
  - PI controller
  - Model Reference Adaptive Controller (MRAC)
  - Generalized Proportional Integral Observer based Robust Controller (GPIRC)

The main reason to include the performance of such classical-advanced control strategies is that the PI controller is well-known and widely used in industry for speed regulation because of its high performance and easy implementation [63]. On the other hand, the MRAC aims to adapt the system parameters periodically by using the closed loop states in order to get the desired response [64]. Finally, the GPIRC is a robust controller that works for a broad class of nonlinear systems [65].

For the simulation test, the proportional and integral gains of the PI controller are set as $K_p^{pi} = 0.03$ and $K_i^{pi} = 7.5$. The adaptation gain of the MRAC is $\Gamma = \mathbf{diag}(2.1 \times 10^4, 6.9 \times 10^2, 8.9 \times 10^{-3}) \in R^{3\times3}$, the P matrix is chosen as $P \in R^{2\times2}$ where $P_{1,1} = 3.1917$, $P_{1,2} = P_{2,1} = 0.0083$, $P_{2,2} =$

Table III: Parameters of the GA and the PSO, which are recurrently used in controller tuning.

Optimizer	pc	η_c	pm	η_m
GA	0.494	0.132	0.783	16.840
Optimizer	C_1	C_2	V_{min}	V_{max}
PSO	0.940	1.990	0.039	0.146

0.0025 and the proportional and derivative gains are selected as $K_p^{mrac} = 600$, $K_d^{mrac} = 200$. The design parameters of the characteristic polynomial associated to the GPI observer in $P_c(s) = \prod_{i=0}^{2}(s^2 + 2h_i\omega_{ni}s + \omega_{ni}^2)$ are set as $\omega_{n0} = 95$, $\omega_{n1} = 130$, $\omega_{n2} = 0.01$, $h_0 = 0.01$, $h_1 = 1$ and $h_2 = 1$, and the observer states use the proportional and derivative gains $K_p^{gpirc} = 2500$ and $K_d^{gpirc} = 200$, respectively.

It is worth to mention that the control parameters of the proposed adaptive control strategy, the bio-inspired adaptive control alternatives, and the classical-advanced control strategies are tuned empirically by a trial and error procedure after an extensive set of runs and the best resulting control parameters are presented above. All control strategies are developed in *C++* programming language in a PC with a 3.60 GHz *i7-4790* processor.

4.2. Simulation results and discussion

In this subsection, the proposed adaptive control strategy based on the IDE is compared with the performance of bio-inspired adaptive control alternatives and classical-advanced control strategies presented in Subsection 4.1.

The bio-inspired adaptive control strategies are tested during 100 inde-

Table IV: Parameter bounds.

Variable	*min*	*max*
$\bar{\theta}_0$	0.1	5.0
$\bar{\theta}_1$	1.0×10^{-3}	5.0×10^{-2}
$\bar{\theta}_2$	1.0×10^{-5}	5.0×10^{-4}

pendent runs. The classical-advanced controllers are tested in a single run because of their deterministic behavior which means that the same error is presented in all runs. The performance of each control system is measured by using three different indicators in the speed error: the Integral Squared Error (ISE), the Integral Absolute Error (IAE) and the Integral Time-weighted Absolute Error (ITAE). Those control measures are computed after the settling period among controllers ($t = 3s$) to perform fair comparisons among them.

Tables V, VI and VII contain the results in simulation of the control systems related with the ISE, IAE and ITAE control measures respectively. Each column represents the best and worst values of those measures, and the mean and standard deviation for all the 100 independent runs of the adaptive control strategy based on the bio-inspired meta-heuristics, respectively. In the case of the classical-advanced controllers, the row data is the same due to the deterministic way to generate the control signal among runs. The boldface results indicate the best value of each column. Moreover, Figs. 4 and 5 show the speed behavior of the DC motor speed for the best run of each control system in the simulation. From the summary of results presented in those tables and figures, different findings are observed:

- The proposed bio-inspired ACS-IDE overcomes all control strategies since it presents the best performance according to the control measures (the ISE, IAE, and ITAE). These measures indicate that the proposal reduces the amplitude of the speed errors over time with less speed error band and less sensitivity to parameter variations through the simulation process.

- The strategies based on the best variants of DE have a better performance than the ones based on the GA and PSO, which are recurrently used in many controller tuning problems.

- Among the bio-inspired control alternatives, the ACS-PSO has the worst performance regarding the ISE, IAE and ITAE indicators and also is the less reliable strategy according to the standard deviation values of these measures. This bad performance can be due to the lack of a selection mechanism (replacement mechanism) in the PSO, which is compensated by using leader solutions but cannot prevent premature convergence to local solutions.

- Concerning the ACS-GA, it has acceptable performance, but due to the less exploitative behavior of the GA (compared with the best variants of DE), more objective function evaluations could be required in order to achieve similar performance to the DE-based controllers. Unlike the GA, the adopted DE variants always use the best solution (this can be the relative best solution in the case of the IDE) to find a suitable search direction, which allows finding good solutions in fewer objective function evaluations with a better exploitative behavior.

- All bio-inspired adaptive controllers improve the speed regulation performance when compared with the classical-advanced controllers. Also, the proportionally small value of the standard deviation of the ISE, IAE, and ITAE measures for the bio-inspired adaptive control systems, shows the reliability of such controllers. In the corresponding figures, it is important to notice that the error produced with bio-inspired adaptive controllers does not exceed the 4% of the reference speed signal when the discontinuous uncertainties are added (in $t \in [4,7]s \bigcup [10,13]s$). As long as continuous perturbations are included, the error level of these strategies is under 1% (in $t \notin [4,7]s \bigcup [10,13]s$).

- Among classical-advanced controllers, the GPIRC presents the largest amplitude of the speed error in an interval of the time (based on the ISE measure), but this is the most stable when the time goes on (based on the IAE and ITAE measures). This indicates that it is sensible to large and discontinuous uncertainties presented in the inertia and friction forces included into the parameters θ_1 and θ_2 of the motor, and this is confirmed in the corresponding figure in the time interval $t \in [10,13]s$, where the GPIRC requires more time to stabilize the motor speed. Nevertheless, this controller is more stable with continuous parameter variations and with discontinuous disturbances ($t \notin [10,13]$). The variation of the speed error from the reference signal in the time interval $t \in [10,13]s$ is around to 6%, 4% and 38% for the PI controller, MRAC and GPIRC, respectively. On the contrary, when the continuous uncertainties are presented in the time interval $t \notin [10,13]s$, the error level is under 3%, 2% and 1%. As it is expected, the linear controller (the PI controller) presents the worst performance for this last case.

- Even when additional dynamics ξ are not considered in the controller used by the ACS-IDE, the IDE can find a suitable set of control parameters $\bar{\theta}^*$ that handles them. In other words, this proposed bio-inspired strategy can compensate the disturbance ξ with the parameters $\bar{\theta}_0$, $\bar{\theta}_1$

and $\bar{\theta}_2$. This behavior is attributed to the search capability of the bio-inspired optimizers.

- Another interesting behavior is observed when the motor is highly disturbed, and the ACS-IDE provides better performance (see Fig. 4 when $t \in [10, 14]s$). This improved performance is due to the form of the search space. With a high perturbation, the number of possible solutions to the optimization problem is decreased and also the number of local solutions, then it is easier for the optimizers to find a global best solution. On the contrary of what can be thought, these perturbations can benefit the performance of the proposed bio-inspired strategy.

It is important to remark that the proposed ACS-IDE, the bio-inspired adaptive control alternatives, the PI controller and the MRAC present a similar energy consumption mean around [0.2032, 0.2048]Wh. Meanwhile, the energy consumption of the GPIRC is $1.475Wh$. Around seven times more energy consumption than the other controllers is required for the GPIRC in order to compensate the discontinuous disturbance in the time interval $[10, 13]s$.

In statistics, when two different samples of a given procedure are subject to random variations (as in the case of bio-inspired adaptive controllers) and cannot be assumed to belong to a normal distribution of probability, is required to use non-parametric tests to make comparisons [66] and to draw formal conclusions.

The non-parametric test of Wilcoxon reveals differences between distributions of two samples and hence identifies if one is better than the other. In this work the Wilcoxon test is used to perform comparisons by pairs among

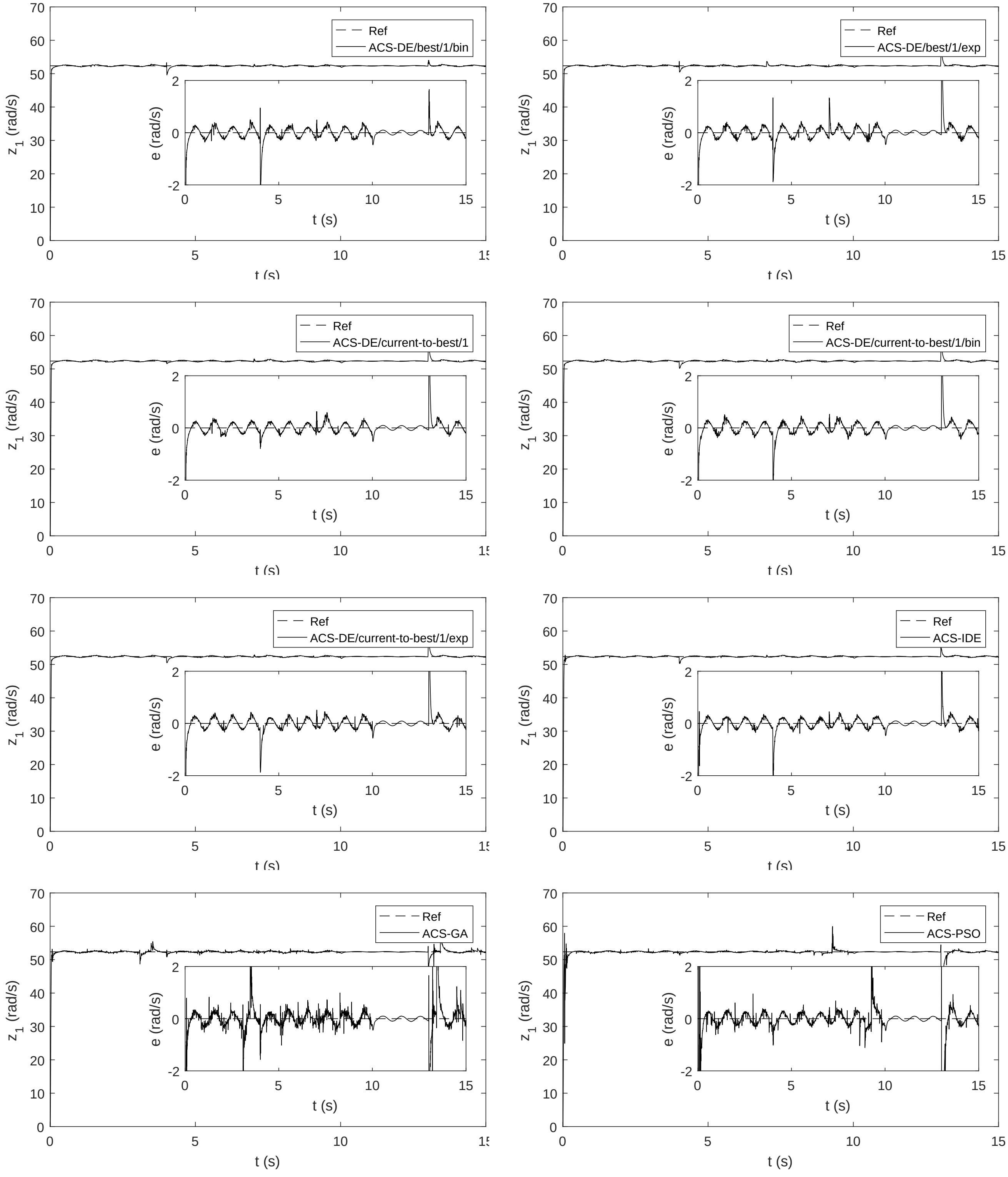

Figure 4: Speed behavior of the best run of the different control systems in simulation (Part I). The speed regulation error (e) is shown in the subplots.

Table V: ISE values for the simulation tests of the different control systems.

Adaptive control strategy alternative	ISE_{best}	ISE_{worst}	$\overline{ISE}$	$std(ISE)$
ACS-DE/best/1/bin	0.392	**0.668**	0.502	**0.071**
ACS-DE/best/1/exp	0.391	1.668	0.684	0.389
ACS-DE/current-to-best/1	0.397	1.446	0.517	0.125
ACS-DE/current-to-best/1/bin	0.399	1.750	0.881	0.464
ACS-DE/current-to-best/1/exp	0.425	1.653	0.810	0.372
ACS-IDE	**0.317**	0.741	**0.440**	0.089
ACS-GA	0.560	4.059	0.927	0.472
ACS-PSO	0.485	16.809	1.923	2.597
PI	22.501	22.501	22.501	0
MRAC	9.704	9.704	9.704	0
GPIRC	64.517	64.517	64.517	0

the performance indicator values ISE, IAE and ITAE of the 100 runs achieved by the bio-inspired adaptive controllers and conclude if one of them performs better than the other. It is important to mention that before performing the Wilcoxon test, the Shapiro-Wilk test is performed in order to check the normality for each pair [67]. The results of the Shapiro-Wilk test show that for almost 90% of the pairs is necessary to use a statistical non-parametric test such as the Wilcoxon one.

Tables VIII, IX and X show the results of the Wilcoxon test for every possible pair. The R_+ value indicates the times that the first alternative overcomes the second one. On the flip side, R_- indicates the times that the

Table VI: IAE values for the simulation tests of the different control systems.

Adaptive control strategy alternative	IAE_{best}	IAE_{worst}	$\overline{IAE}$	$std(IAE)$
ACS-DE/best/1/bin	1.686	1.933	1.810	0.058
ACS-DE/best/1/exp	1.679	2.186	1.864	0.117
ACS-DE/current-to-best/1	1.714	2.002	1.819	0.065
ACS-DE/current-to-best/1/bin	1.697	2.168	1.907	0.131
ACS-DE/current-to-best/1/exp	1.729	2.165	1.912	0.110
ACS-IDE	**1.575**	**1.838**	**1.681**	**0.056**
ACS-GA	2.012	3.153	2.244	0.158
ACS-PSO	1.850	3.510	2.189	0.308
PI	14.261	14.261	14.261	0
MRAC	9.401	9.401	9.401	0
GPIRC	7.424	7.424	7.424	0

second alternative overcomes the first one. The $p-value$ denotes the probability of accepting the *null* hypothesis which establishes that a pair of samples has the same distribution. Then, $p-value$ is also related with the statistical significance of the test, so values under a reasonable percentage (typically 5% or 10%) allow the rejection of the *null* hypothesis and the acceptance of the alternative hypothesis. For the performed tests, the statistical significance is set to 5% and the *two-sided* alternative hypothesis is selected. The *two-sided* hypothesis establishes that two samples have different distributions and in that case, the R_+ and R_- values reveal the location of each distribution. In Tables VIII, IX and X, the winner of each test is shown in boldface. Table

Table VII: ITAE values for the simulation tests of the different control systems.

Adaptive control strategy alternative	$ITAE_{best}$	$ITAE_{worst}$	$\overline{ITAE}$	$std(ITAE)$
ACS-DE/best/1/bin	14.314	15.925	15.221	**0.347**
ACS-DE/best/1/exp	14.371	19.384	15.840	1.302
ACS-DE/current-to-best/1	14.382	17.819	15.333	0.497
ACS-DE/current-to-best/1/bin	14.503	19.230	16.494	1.565
ACS-DE/current-to-best/1/exp	14.699	19.277	16.458	1.249
ACS-IDE	**13.407**	**15.783**	**14.305**	0.496
ACS-GA	16.830	29.215	18.969	1.650
ACS-PSO	15.536	36.212	19.166	3.768
PI	130.612	130.612	130.612	0
MRAC	83.756	83.756	83.756	0
GPIRC	73.950	73.950	73.950	0

XI summarizes the overall results of the performed Wilcoxon test. According to the number of wins, the best performing alternative turned out to be the ACS-IDE and is followed by the ACS-DE/best/1/bin, ACS-DE/current-to-best/1, ACS-DE/best/1/exp, ACS-DE/current-to-best /1/bin, and ACS-DE/current-to-best/1/exp, ACS-GA and ACS-PSO in that order.

Based on the statistical evidence of results in simulation, the ACS-IDE proved to have the best performance. Then, the ACS-IDE is a suitable alternative for the problem of the speed regulation task of the DC motor when there are parametric uncertainties, and its performance is tested next for the experimental stage.

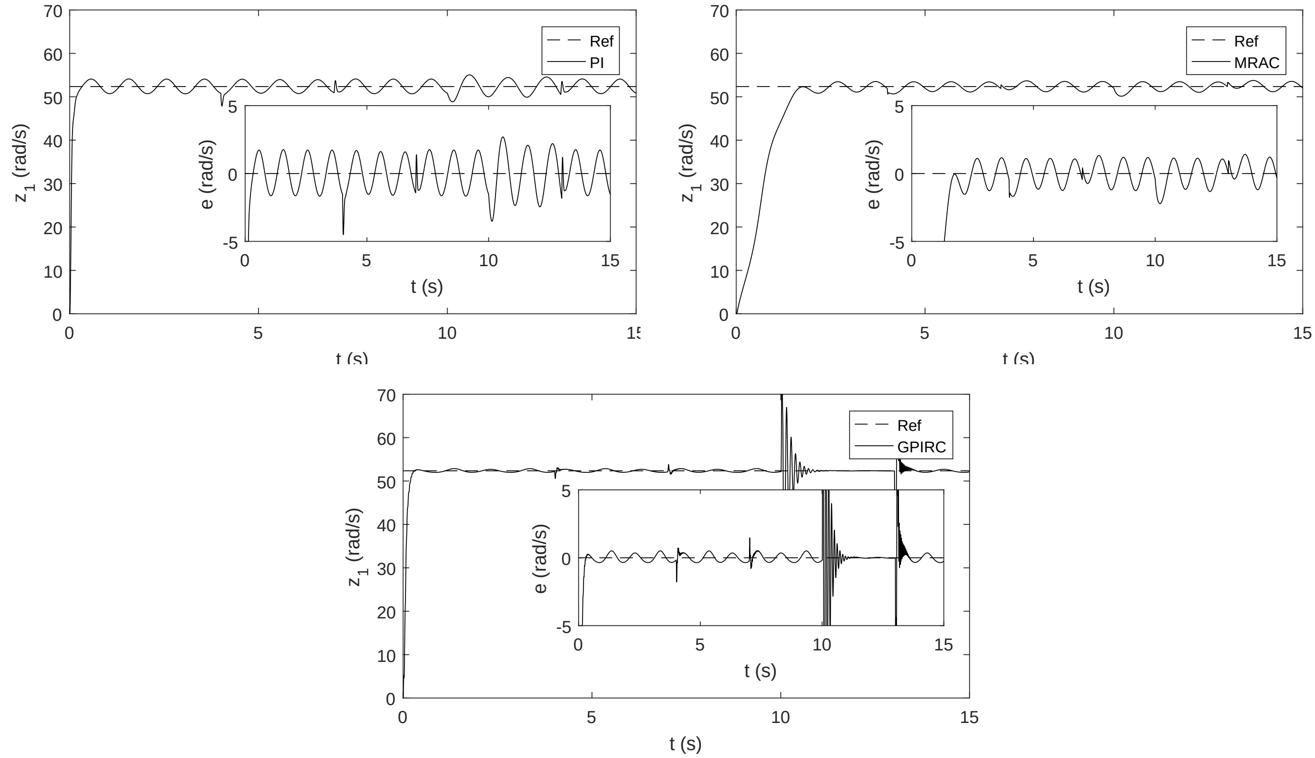

Figure 5: Speed behavior of the best run of the different control systems in simulation (Part II). The speed regulation error (e) is shown in the subplots.

4.3. Experiment details

The complete experimental prototype is illustrated in Fig. 6 and the closed-loop system is shown in Fig. 7. The experimental prototype uses a PC with a 3.60 GHz *i7-4790* processor with a data acquisition board *Sensoray 626* to get the angular position of the motor from a rotary encoder BEI E25BB. The angular speed and acceleration of the motor are estimated. The output control signal, computed in the PC, is sent to the servo-amplifier *25A8B-GAL* through the analog output of the acquisition board. This servo-amplifier requires an external power source of $48V/6A$. The amplified signal is finally used to control the permanent magnet DC motor *MET 3B-9013182D* which is assembled with the disturbance mechanism. This mechanism is shown in Fig. 6 and is designed to add some friction and inertia to the DC motor by incorporating a solid iron disk with a mass of $1.64Kg$ and an inertia of 0.00297 Nms^2.

The real-time implementation of the proposed adaptive control strategy is shown in Fig. 8. In this, a *Sensoray 626* timer configured with a frequency of 200 Hz (i.e., with a period of 5ms), is used as the real-time clock. The timer periodically triggers a high priority software interruption which is handled by the PC with an execution thread. This thread is responsible for acquiring the motor states and computing the corresponding control signal, as well as update the optimization problem to find the best control parameters.

The interruption thread tasks are detailed next:

1. **Get angular position**: Reads the counter register of the *Sensoray 626* board which counts the pulses of the rotary encoder. This information is then used to compute the angular position of the DC motor by dividing the count by the linear resolution of the encoder as $q(t) = 2\pi \frac{count}{resolution}$.
2. **Estimate angular speed**: Estimates the angular speed of the DC motor by using the symmetric difference quotient $\hat{z}_1(t) = \frac{q(t+\triangle t)-q(t-\triangle t)}{2\triangle t}$.
3. **Filter angular speed**: Filters the angular speed of the DC motor by using a Kalman Filter $z_1(t) = \dot{q}(t) = K_k\hat{z}_1(t)+(1-K_k)z_1(t-\triangle t)$ where the Kalman gain K_k obtained from [68], with $Q = 0.1$ and $R = 0.9$, is used in order to decrease the noise added by the symmetric difference quotient.
4. **Estimate the angular acceleration**: Estimates the angular acceleration of the DC motor by using the symmetric difference quotient $z_2(t) = \ddot{q}(t) = \frac{\dot{q}(t+\triangle t)-\dot{q}(t-\triangle t)}{2\triangle t}$.
5. **Store states**: Stores the current states $z = [z_1, z_2]^T$ in memory.

6. **Update control signal**: Computes and stores the corresponding control signal $u(t)$ by using the current motor states $z(t)$ and the last found control parameters $\theta(t)$. This control signal is first transformed to a digital value by $u^d = \lfloor u \frac{resolution}{max\ voltage} \rfloor$, with the *Sensoray 626* DAC converter resolution of $2^{13} - 1$ and the maximum servo-amplifier output of 48V are taken into account. Then, u^d is sent to the DAC register of the *Sensoray 626* board and is transformed to an analog signal in $[-10, 10]V$ which feeds the DC motor servo-amplifier.

7. **Update optimization problem**: Updates the optimization problem by taking into account the stored states and control signals within the past time interval Ω.

8. **Run optimizer**: Runs the IDE algorithm to find the most suitable controller parameters. It is important to mention that this optimization process takes at most $1.5ms$.

9. **Update controller parameters**: Replaces the controller parameters with those obtained from the optimization process.

For the experimental results the ACS-IDE and the classical-advanced control strategies are compared. The conditions for the experimentation are similar to those presented in Subsection 4.1. The main differences are described below:

- The tests are performed during $10s$ with the same sampling time $\Delta t = 5ms$ and the only considered perturbation is the change of the DC motor load in $t \in [4, 8]s$ which modifies its friction and inertia parameters, i.e., for each experimental test, the iron disk of the disturbance mechanism is added to the motor when $t = 4s$ and is removed when $t = 8s$.

- The inverse dynamic controller gains are set as $K_p^{acs} = 800$ and $K_d^{acs} = 55$.

- The search space of the optimization problem for the ACS-IDE is bounded according to the Table XII. As an authors suggestion, in order to establish the bounds of the search space for the experimental setup, the difference value between $\bar{\theta}_{i,max}$ and $\bar{\theta}_{i,min}$ must be approximately equal to the nominal value θ_i (this can be obtained from the manufacturer specification or from an identification process). For the parameters $\bar{\theta}_0$ and $\bar{\theta}_1$, it is recommended that their interval $[\bar{\theta}_{i,min}, \bar{\theta}_{i,max}]$ includes their nominal values given by θ_0 and θ_1 in the middle of it. In the case of $\bar{\theta}_2$, it is suggested that its lower bound $\bar{\theta}_{2,min}$ be over the 25% of its nominal value θ_2.

- The adaptation gain of the MRAC is $\Gamma = \mathbf{diag}(1.0\times10^4, 6.9\times10^2, 1.0\times10^{-3}) \in R^{3\times3}$.

- The parameters of the GPIRC controller are set as $\omega_{n0} = 1.7$, $\omega_{n1} = 0.25$, $\omega_{n2} = 1.7$, $h_0 = 0.01$, $h_1 = 2.2$ and $h_2 = 0.01$, and its PD controller gains as $K_p^{gpirc} = 3500$, $K_d^{gpirc} = 200$.

The remaining conditions for the experimental tests, in the parameters of the ACS-IDE and classical-advanced control strategies, are the same as described in Subsection 4.1.

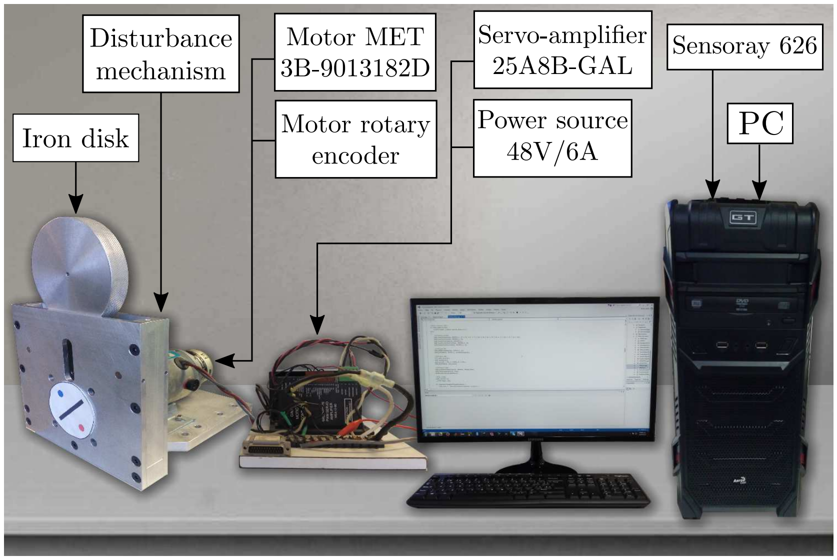

Figure 6: Experimental prototype.

The parameters of all control systems are obtained through an arduous process of trial and error tests.

4.4. Experiment results and discussion

The ACS-IDE strategy and classical-advanced controllers are experimentally tested during 25 independent runs. Even when the PI controller, the MRAC and the GPIRC have deterministic behavior, it is necessary to perform several runs over them since any experimental test implicitly includes the stochastic behavior of the input and output signals due to noised electrical measurements.

First, the response characteristics based on the raise time (RT), overshoot (OS), settling time (ST), and steady-state error (SSE) are evaluated for the 25 independent runs of each controller. Table XIII shows the mini-

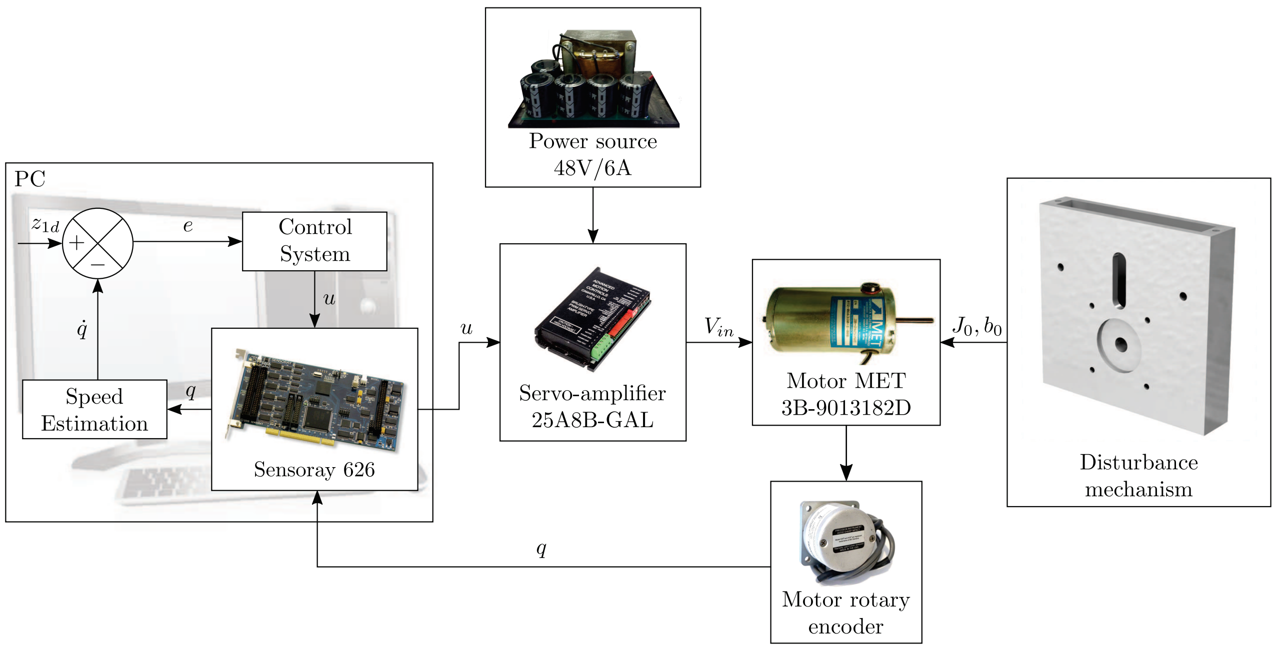

Figure 7: Block diagram of the closed loop system.

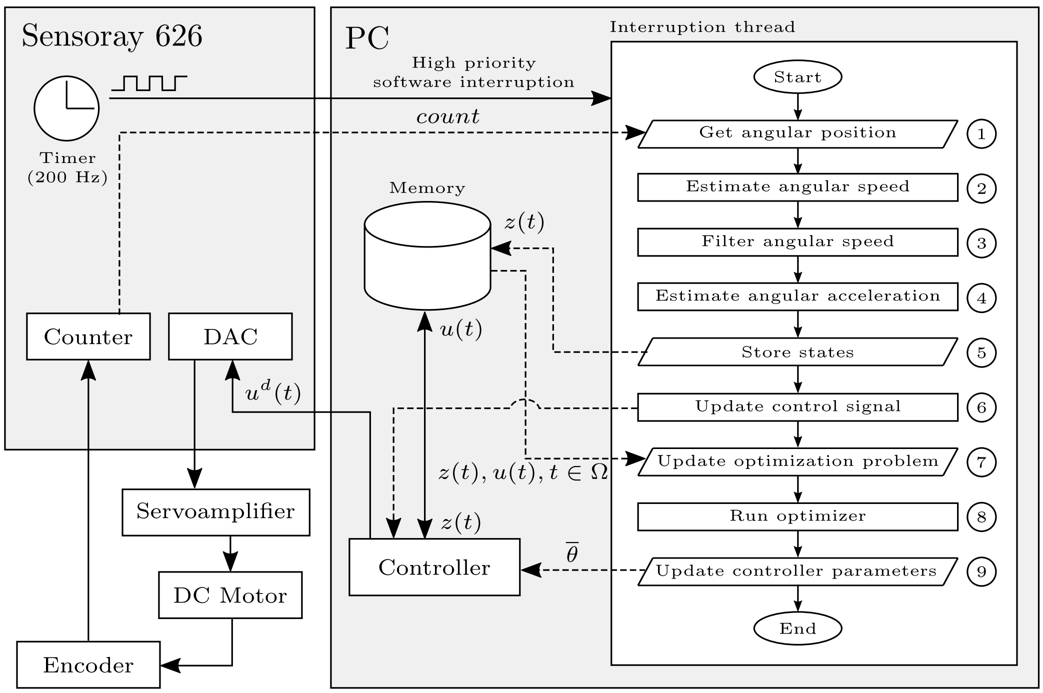

Figure 8: Real-time implementation diagram.

mum, maximum, and mean values of such characteristics. According to this table, the proposal ACS-IDE has an outstanding performance regarding the RT and SSE indicators when compared with the other control alternatives, i.e., the ACS-IDE can reach the speed profile in a shorter time and is less susceptible to steady-state errors. Concerning the OS indicator, the MRAC can reach the speed profile without exceeding it abruptly, but the above fact is contrasted with the larger time required to reach the steady-state denoted by ST. Regarding the ST, the PI controller and the ACS-IDE have the most competitive performance.

Then, the ISE, IAE and ITAE measures are considered to make comparisons in order to show the advantages of the proposal. These control measures are obtained in the interval of time $t \in [3.5, 10]s$ in order to perform fair comparisons. This interval is proposed according to the time required for the MRAC to regulate the DC motor speed to the reference signal.

Tables XIV, XV and XVI show the values of the ISE, IAE and ITAE, respectively. The $\overline{ISE}$ column in Table XIV shows that the ACS-IDE has a significantly better performance than the rest of alternatives, i.e., the ACS-IDE is the least susceptible to large errors. Taking into account the values of $\overline{IAE}$ and $\overline{ITAE}$ columns in Tables XV and XVI respectively, the performances of the ACS-IDE and the MRAC are both competitive and are over the performance of the PI controller and the GPIRC, then those controllers produce a less oscillating speed signal along all the experiment execution time.

The speed behavior of the best run of the ACS-IDE, the PI controller, the MRAC and the GPIRC according to the ISE indicator, is observed in

Fig. 9. The error band of all alternatives does not surpass the 0.2% from the reference signal when the motor is not disturbed and does not surpass the 4% when the disk is added. In Fig. 9, the ACS-IDE, and MRAC are better than the PI controller and the GPIRC for the proposed experimental conditions. The error signal, obtained by the ACS-IDE and the MRAC, is almost equally bounded when the system is disturbed. Nevertheless, the error signal of the ACS-IDE is attenuated, i.e., the motor speed is closer to the reference signal in several instants during the experiment execution, so this proposal provides a better parameter adaptation. On the other hand, all control alternatives have a very similar energy consumption.

Although the previous descriptive parametric statistical analysis presents a summary of the obtained data, the use of non-parametric statistics is necessary since the experiment presents some unavoidable conditions such as state noise and mechanical vibrations due to the disturbance mechanism movements when adding the iron disk. For this reason, the non-parametric test of Wilcoxon is applied by pairs to the distributions of the ISE, IAE and ITAE measures of the 25 independent runs of the ACS-IDE, the PI controller, the MRAC and the GPIRC. Tables XVII, XVIII and XIX show the results of each Wilcoxon test where the winner alternative of each pair is shown in boldface. Table XX contains the overall wins of the performed Wilcoxon tests. As it can be seen in Table XX, the ACS-IDE alternative is the most promising when the ISE, the IAE, and the ITAE performance control measures are considered. The next promising control alternatives are the MRAC, the PI controller and the GPIRC in this order.

The statistical evidence over the experimental tests presented in this sub-

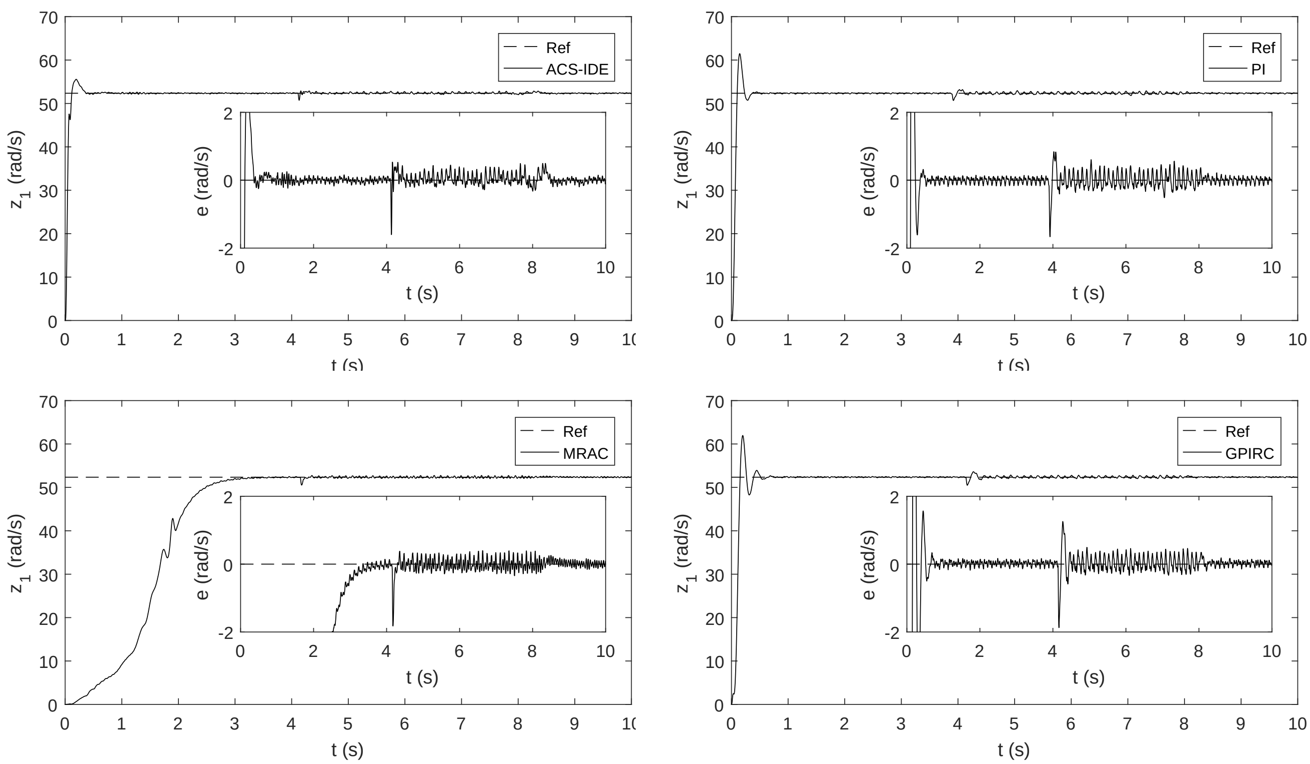

Figure 9: Speed behavior of the best runs in experimentation of the proposed control strategy based on the IDE, the PI controller, the MRAC and the GPIRC according to the ISE indicator. The speed regulation error (e) is shown in the subplots.

section, reveals that the ACS-IDE is capable of dealing with real parametric uncertainties and presents performance advantages over some classical-advanced control approaches.

5. Conclusion and future work

In this work, an adaptive control strategy based on an improved version of DE (ACS-IDE) is proposed for the highly efficient speed regulation of the DC motor when there are parametric uncertainties. For this strategy, an optimization problem is stated and solved online at each sampling time by IDE to obtain an optimal set of parameters that are used in calculating the control signal. ACS-IDE includes a mechanism that promotes the exploration in the early generations and takes advantage of the exploitation power of the DE/best class in the last generations of the algorithm.

The following conclusions can be drawn based on the results in simulation and experimentation with a real prototype:

- The effectiveness and stability of the proposed bio-inspired adaptive control strategy is proven from control theory and then validated in simulation and experimentation through a descriptive and non-parametric statistical analysis.
- The proposed ACS-IDE shows to have a promising performance in the speed control of the DC motor subject to uncertainties in simulation and experimentation.
- Statistical evidence of the simulation test reveals that ACS-IDE performs better than several strategies based on five different best vari-

ants of DE (ACS-DE/best/1/bin, ACS-DE/current-to-best/1, ACS-DE/best/1/exp, ACS-DE/current-to-best/1/bin, and ACS-DE/current-to-best/ 1/exp) and two well-known meta-heuristic optimizers, the GA and PSO (ACS-GA and ACS-PSO). The above performance improvement of ACS-IDE is attributed to the balanced trade-off between the exploration and exploitation capabilities of IDE, while in the rest of the adopted optimizers, one capability stands out from the other. The lack of exploration of the five variants of DE and the PSO make these optimizers more susceptible to converge or stuck in local solutions. In the case of the GA, the lack of exploitation slows the search for fine promising solutions, i.e., more objective function evaluations may be required to achieve better performance.

- Results in simulation also reveal an outstanding performance of ACS-IDE concerning three classical-advanced controllers (the PI controller, MRAC and GPIRC), especially when the motor parameters present large discontinuous uncertainties which reduce the number of local solutions to the optimization problem and facilitate the search for good solutions with IDE.

- The proposed ACS-IDE is almost equally competitive to the three classical-advanced controllers in experimentation when there are no uncertainties, but when the DC motor is abruptly disturbed (by adding the iron disk), the benefits in performance when using ACS-IDE can be observed through a descriptive and non-parametric statistical analysis.

- Some significant advantages of the ACS-IDE include its faster adaptation capability under uncertainties, the short time of $\triangle w$ to get the first set of suitable control parameters and the possibility to compensate the variations of unknown parametric uncertainties.

- The main difficulty in the use of ACS-IDE is the statement of the bounds of the search space and the tuning of the gains K_p^{acs} and K_d^{acs}. In order to select the correct parameter bounds in ACS-IDE, it is necessary to take into account the nominal values of the DC motor parameters. Since this information is not always available, it is required to perform an initial identification process. A similar situation is observed with the gains K_p^{acs} and K_d^{acs}, whose values are related to the bounds of the motor parameters.

As the future work, a multi-objective problem could be stated considering several performance indicators to satisfy different control engineering necessities. Moreover, a study of multi-objective optimizers from different search approaches based on Pareto dominance, decomposition and performance metrics in the adaptive control problem is suggested. A study of high-performance computing techniques to increase the efficiency of the IDE optimizer for its application in the control of different complex dynamic systems is also proposed.

Acknowledgments

The authors acknowledge the support of the Secretaría de Investigación y Posgrado (SIP) through the projects No. SIP-20172317 and No. SIP-20180637; and of the Consejo Nacional de Ciencia y Tecnología (CONACyT) under the projects 182298 and 254329. The first author acknowledges the support from the Consejo Nacional de Ciencia y Tecnología (CONACyT) through the scholarship to pursue his graduate studies at CIDETEC-IPN.

References

[1] C. Guo-qiang, Z. Zhi-rui, Mechanical analysis of the industrial robot to upgrade to the gaming robot, Procedia Engineering 174 (2017) 1077 – 1083.

[2] A. Derdiyok, B. Soysal, F. Arslan, Y. Ozoglu, M. Garip, An adaptive compensator for a vehicle driven by dc motors, Journal of the Franklin Institute 342 (3) (2005) 273 – 283.

[3] T. Szecsi, A dc motor based cutting tool condition monitoring system, Journal of Materials Processing Technology 92 (1999) 350 – 354.

[4] P. M. Meshram, R. G. Kanojiya, Tuning of pid controller using ziegler-nichols method for speed control of dc motor, in: IEEE-International Conference On Advances In Engineering, Science And Management (ICAESM -2012), 2012, pp. 117–122.

[5] Y. Wang, D. J. Hill, G. Guo, Robust decentralized control for multi-machine power systems, IEEE Transactions on Circuits and Systems I: Fundamental Theory and Applications 45 (3) (1998) 271–279.

[6] S. Al-Hiddabi, B. Samanta, A. Seibi, Non-linear control of torsional and bending vibrations of oilwell drillstrings, Journal of Sound and Vibration 265 (2) (2003) 401 – 415.

[7] N. C. Chen, P. He, X. Yu, Application of the LMI approach in the robust force control of servo-hydraulic actuator with parametric uncertainties, in: Applied Mechanics And Mechanical Engineering, 2010, pp. 240–245.

[8] K. Liu, Y. Yao, Robust Control: Theory and Applications, Wiley, 2016.

[9] B. Pal, B. Chaudhuri, Robust Control in Power Systems, Power Electronics and Power Systems, Springer US, 2006.

[10] Q. Song, C. Jia, Robust speed controller design for permanent magnet synchronous motor drives based on sliding mode control, Energy Procedia 88 (2016) 867 – 873.

[11] K. H. Kim, I. C. Baik, S. K. Chung, M. J. Youn, Robust speed control of brushless dc motor using adaptive input-output linearisation technique, IEE Proceedings - Electric Power Applications 144 (6) (1997) 469–475.

[12] J. Linares-Flores, J. L. Barahona-Avalos, H. Sira-Ramirez, M. A. Contreras-Ordaz, Robust Passivity-Based Control of a Buck-Boost-Converter/DC-Motor System: An Active Disturbance Rejection Approach, IEEE Transactions on Industry Applications 48 (6) (2012) 2362–2371.

[13] R. G. Orozco, E. I. Jimenez, M. Jimenez-Lizarraga, Comparative study of the speed robust control of a dc motor, in: World Automation Congress 2012, 2012, pp. 1–6.

[14] W. Zheng, Y. Pi, Study of the fractional order proportional integral controller for the permanent magnet synchronous motor based on the differential evolution algorithm, ISA Transactions 63 (2016) 387 – 393.

[15] A. Moharam, M. A. El-Hosseini, H. A. Ali, Design of optimal pid controller using hybrid differential evolution and particle swarm optimization with an aging leader and challengers, Applied Soft Computing 38 (2016) 727 – 737.

[16] M. G. Villarreal-Cervantes, J. Alvarez-Gallegos, Off-line PID control tuning for a planar parallel robot using DE variants, Expert Systems with Applications 64 (Supplement C) (2016) 444 – 454.

[17] E. S. Ali, Speed control of dc series motor supplied by photovoltaic system via firefly algorithm, Neural Computing and Applications 26 (6) (2015) 1321–1332.

[18] A. Oshaba, E. Ali, S. A. Elazim, Aco based speed control of srm fed by photovoltaic system, International Journal of Electrical Power & Energy Systems 67 (2015) 529 – 536.

[19] E. S. Ali, Speed control of induction motor supplied by wind turbine via imperialist competitive algorithm, Energy 89 (2015) 593 – 600.

[20] D. Thangavelusamy, L. Ponnusamy, Comparison of pi controller tuning using ga and pso for a multivariable experimental four tank system, International Journal of Engineering and Technology (IJET) 5 (6) (2014) 4660–4671.

[21] B. Nagaraj, N. Murugananth, A comparative study of pid controller tuning using ga, ep, pso and aco, in: 2010 International Conference on Communication Control and Computing Technologies, 2010, pp. 305–313.

[22] I. Landau, R. Lozano, M. M'Saad, Adaptive Control: Algorithms, Analysis and Applications, Springer Science+Business Media, New York, NY, USA, 2011.

[23] C. Tan, H. Yang, G. Tao, A multiple-model mrac scheme for multivariable systems with matching uncertainties, Information Sciences 360 (2016) 217 – 230.

[24] J. Mo, Z. Qiu, J. Wei, X. Zhang, Adaptive positioning control of an ultrasonic linear motor system, Robotics and Computer-Integrated Manufacturing 44 (2017) 156 – 173.

[25] H. Asare, D. Wilson, Evaluation of three model reference adaptive control algorithms for robotic manipulators, in: Proceedings. 1987 IEEE International Conference on Robotics and Automation, Vol. 4, 1987, pp. 1531–1542.

[26] J. P. Hespanha, D. Liberzon, A. Morse, Overcoming the limitations of adaptive control by means of logic-based switching, Systems & Control Letters 49 (1) (2003) 49 – 65, adaptive Control.

[27] H.-C. Lu, M.-H. Chang, C.-H. Tsai, Parameter estimation of fuzzy neural network controller based on a modified differential evolution, Neurocomputing 89 (2012) 178 – 192.

[28] L. Tang, J. Zhao, Neural network based adaptive prescribed performance control for a class of switched nonlinear systems, Neurocomputing 230 (2017) 316 – 321.

[29] L. O. A. P. Henriques, P. J. C. Branco, L. G. B. Rolim, W. I. Suemitsu, Proposition of an offline learning current modulation for torque-ripple reduction in switched reluctance motors: design and experimental evaluation, IEEE Transactions on Industrial Electronics 49 (3) (2002) 665–676.

[30] E. Ramadan, M. El-bardini, M. Fkirin, Design and FPGA-implementation of an improved adaptive fuzzy logic controller for DC motor speed control, Ain Shams Engineering Journal 5 (3) (2014) 803 – 816.

[31] K. Bedoud, M. Ali-rachedi, T. Bahi, R. Lakel, Adaptive fuzzy gain scheduling of PI controller for control of the wind energy conversion systems, Energy Procedia 74 (2015) 211 – 225.

[32] K. Premkumar, B. Manikandan, Speed control of brushless dc motor using bat algorithm optimized adaptive neuro-fuzzy inference system, Applied Soft Computing 32 (2015) 403 – 419.

[33] K. Premkumar, B. V. Manikandan, C. A. Kumar, Antlion algorithm optimized fuzzy pid supervised on-line recurrent fuzzy neural network based controller for brushless dc motor, Electric Power Components and Systems 45 (20) (2017) 2304–2317.

[34] S. Rao, Engineering Optimization: Theory and Practice: Fourth Edition, John Wiley and Sons, 2009.

[35] W. Sun, Y. Yuan, Optimization Theory and Methods: Nonlinear Programming, 1st Edition, Vol. 1, Springer, 2006.

[36] M. Gilli, D. Maringer, E. Schumann, Numerical Methods and Optimization in Finance, 1st Edition, Vol. 1, Academic Press, 2011.

[37] D. E. Goldberg, Genetic Algorithms in Search, Optimization and Machine Learning, 1st Edition, Vol. 1, Addison-Wesley, 1989.

[38] F. Lin, H. Shieh, K. Shyu, P. Huang, On-line gain-tuning IP controller using real-coded genetic algorithm, Electric Power Systems Research 72 (2) (2004) 157 – 169.

[39] S. García, A. Fernández, J. Luengo, F. Herrera, A study of statistical techniques and performance measures for genetics-based machine learning: accuracy and interpretability, Soft Computing 13 (10) (2008) 959.

[40] A. Rodríguez-Molina, M. Villarreal-Cervantes, M. Aldape-Pérez, An adaptive control study for the DC motor using meta-heuristic algorithms, Soft Computing (2017) 1–18.

[41] S. Das, A. Mandal, R. Mukherjee, An adaptive differential evolution algorithm for global optimization in dynamic environments, IEEE Transactions on Cybernetics 44 (6) (2014) 966–978.

[42] K. Deb, D. Kalyanmoy, Multi-Objective Optimization Using Evolutionary Algorithms, John Wiley & Sons, Inc., New York, NY, USA, 2001.

[43] C. B. Reeves, Sons, Modern Heuristic Techniques for Combinatorial Problems, 1st Edition, Vol. 1, Wiley, 1993.

[44] D. H. Wolpert, W. G. Macready, No free lunch theorems for optimization, IEEE transactions on evolutionary computation 1 (1) (1997) 67–82.

[45] K. Price, R. M. Storn, J. A. Lampinen, Differential Evolution: A Practical Approach to Global Optimization (Natural Computing Series), Springer-Verlag New York, Inc., Secaucus, NJ, USA, 2005.

[46] L. M. Zheng, S. X. Zhang, K. S. Tang, S. Y. Zheng, Differential evolution powered by collective information, Information Sciences 399 (2017) 13 – 29.

[47] S. Das, P. N. Suganthan, Differential evolution: A survey of the state-of-the-art, IEEE Transactions on Evolutionary Computation 15 (1) (2011) 4–31.

[48] M. G. Villarreal-Cervantes, C. A. Cruz-Villar, J. Alvarez-Gallegos, Synergetic structure–control design via a hybrid gradient-evolutionary algorithm, Optimization and Engineering 16 (3) (2015) 511–539.

[49] E. J. Hughes, Multi-objective binary search optimisation, in: Evolutionary Multi-Criterion Optimization: Second International Conference, EMO 2003. Proceedings, Springer Berlin Heidelberg, Berlin, Heidelberg, 2003, pp. 102–117.

[50] M. Cárdenas-Montes, Incorporating more scaled differences to differential evolution, in: Hybrid Artificial Intelligent Systems: 12th International Conference, HAIS 2017. Proceedings, Springer International Publishing, 2017, pp. 101–112.

[51] A. Qing, C. K. Lee, Differential Evolution in Electromagnetics, 1st Edition, Springer Publishing Company, Incorporated, 2010.

[52] S. Sivanandam, S. Deepa, Introduction to Genetic Algorithms, Springer Berlin Heidelberg, Berlin, Heidelberg, 2008.

[53] E. Mezura-Montes, J. Velázquez-Reyes, C. A. Coello, A comparative study of differential evolution variants for global optimization, in: Proceedings of the 8th Annual Conference on Genetic and Evolutionary Computation, 2006, pp. 485–492.

[54] K. Deb, An efficient constraint handling method for genetic algorithms, in: Computer Methods in Applied Mechanics and Engineering, 2000, pp. 311–338.

[55] P. Fleming, R. Purshouse, Evolutionary algorithms in control systems engineering: a survey, Control Engineering Practice 10 (11) (2002) 1223 – 1241.

[56] V. Pano, P. R. Ouyang, Gain tuning of position domain pid control using particle swarm optimization, Robotica 34 (6) (2016) 1351–1366.

[57] T. Eswaran, V. S. Kumar, Particle swarm optimization (pso)-based tuning technique for pi controller for management of a distributed static synchronous compensator (dstatcom) for improved dynamic response and power quality, Journal of Applied Research and Technology 15 (2) (2017) 173 – 189.

[58] M. Tian, X. Gao, C. Dai, Differential evolution with improved individual-based parameter setting and selection strategy, Applied Soft Computing 56 (2017) 286 – 297.

[59] K. Deb, R. B. Agrawal, Simulated binary crossover for continuous search space, Complex Systems 9 (3) (1994) 1–15.

[60] K. Deb, D. Deb, Analysing mutation schemes for real-parameter genetic algorithms, International Journal of Artificial Intelligence and Soft Computing 4 (1) (2014) 1–28.

[61] A. Kaveh, Particle Swarm Optimization, Springer International Publishing, Cham, 2017, pp. 11–43.

[62] J. C. Bansal, P. Singh, M. Saraswat, A. Verma, S. S. Jadon, A. Abraham, Inertia weight strategies in particle swarm optimization, in: Nature and Biologically Inspired Computing (NaBIC), 2011 Third World Congress on, IEEE, 2011, pp. 633–640.

[63] T.-C. Chen, T.-T. Sheu, Model reference neural network controller for induction motor speed control, IEEE Transactions on Energy Conversion 17 (2) (2002) 157–163.

[64] G. Wu, S. Wu, Y. Bai, L. Liu, Experimental studies on model reference adaptive control with integral action employing a rotary encoder and tachometer sensors, Sensors 13 (2013) 4742–4759.

[65] H. Sira-Ramirez, A. Luviano-Juárez, J. Cortés-Romero, Control lineal robusto de sistemas no lineales diferencialmente planos, Revista Iberoamericana de Automática e Informática Industrial RIAI 8 (1) (2011) 14 – 28.

[66] J. Derrac, S. García, D. Molina, F. Herrera, A practical tutorial on the use of nonparametric statistical tests as a methodology for comparing

evolutionary and swarm intelligence algorithms, Swarm and Evolutionary Computation 1 (1) (2011) 3 – 18.

[67] M. I. Rodrigues, A. F. Iemma, Experimental Design and Process Optimization, 1st Edition, CRC Press, 2014.

[68] G. Roşu, R. P. Venkatesan, J. Whittle, L. Leuştean, Certifying optimality of state estimation programs, in: Computer Aided Verification: 15th International Conference, 2003, pp. 301–314.

Table VIII: Results of the Wilcoxon test over the ISE values achieved in simulation by the proposed adaptive control strategies.

Test	R_+	R_-	$p-value$
ACS-DE/best/1/bin vs ACS-DE/best/1/exp	3494	1556	0.0008
ACS-DE/best/1/bin vs ACS-DE/current-to-best/1	2685	2365	0.5849
ACS-DE/best/1/bin vs ACS-DE/current-to-best/1/bin	4307	743	<0.0001
ACS-DE/best/1/bin vs ACS-DE/current-to-best/1/exp	4542	508	<0.0001
ACS-DE/best/1/bin vs ACS-GA	5050	0	<0.0001
ACS-DE/best/1/bin vs **ACS-IDE**	1131	3919	<0.0001
ACS-DE/best/1/bin vs ACS-PSO	5007	43	<0.0001
ACS-DE/best/1/exp vs **ACS-DE/current-to-best/1**	1760	3290	0.0081
ACS-DE/best/1/exp vs ACS-DE/current-to-best/1/bin	3328	1722	0.0054
ACS-DE/best/1/exp vs ACS-DE/current-to-best/1/exp	3325	1725	0.0056
ACS-DE/best/1/exp vs ACS-GA	3893	1157	<0.0001
ACS-DE/best/1/exp vs **ACS-IDE**	613	4437	<0.0001
ACS-DE/best/1/exp vs ACS-PSO	4242	808	<0.0001
ACS-DE/current-to-best/1 vs ACS-DE/current-to-best/1/bin	4209	841	<0.0001
ACS-DE/current-to-best/1 vs ACS-DE/current-to-best/1/exp	4420	630	<0.0001
ACS-DE/current-to-best/1 vs ACS-GA	4961	89	<0.0001
ACS-DE/current-to-best/1 vs **ACS-IDE**	973	4077	<0.0001
ACS-DE/current-to-best/1 vs ACS-PSO	4958	92	<0.0001
ACS-DE/current-to-best/1/bin vs ACS-DE/current-to-best/1/exp	2137	2913	0.1835
ACS-DE/current-to-best/1/bin vs ACS-GA	2575	2475	0.8654
ACS-DE/current-to-best/1/bin vs **ACS-IDE**	268	4782	<0.0001
ACS-DE/current-to-best/1/bin vs ACS-PSO	3517	1533	0.0005
ACS-DE/current-to-best/1/exp vs ACS-GA	3089	1961	0.0524
ACS-DE/current-to-best/1/exp vs **ACS-IDE**	318	4732	<0.0001
ACS-DE/current-to-best/1/exp vs ACS-PSO	3867	1183	<0.0001
ACS-GA vs **ACS-IDE**	3	5047	<0.0001
ACS-GA vs ACS-PSO	3287	1763	0.0084
ACS-IDE vs ACS-PSO	5038	12	<0.0001

Table IX: Results of the Wilcoxon test over the IAE values achieved in simulation by the proposed adaptive control strategies.

Test	R_+	R_-	$p-value$
ACS-DE/best/1/bin vs ACS-DE/best/1/exp	3526	1524	0.0004
ACS-DE/best/1/bin vs ACS-DE/current-to-best/1	2878	2172	0.2255
ACS-DE/best/1/bin vs ACS-DE/current-to-best/1/bin	4251	799	<0.0001
ACS-DE/best/1/bin vs ACS-DE/current-to-best/1/exp	4460	590	<0.0001
ACS-DE/best/1/bin vs ACS-GA	5050	0	<0.0001
ACS-DE/best/1/bin vs **ACS-IDE**	65	4985	<0.0001
ACS-DE/best/1/bin vs ACS-PSO	5042	8	<0.0001
ACS-DE/best/1/exp vs **ACS-DE/current-to-best/1**	1825	3225	0.0161
ACS-DE/best/1/exp vs ACS-DE/current-to-best/1/bin	3219	1831	0.01665
ACS-DE/best/1/exp vs ACS-DE/current-to-best/1/exp	3342.5	1707.5	0.0049
ACS-DE/best/1/exp vs ACS-GA	5050	0	<0.0001
ACS-DE/best/1/exp vs **ACS-IDE**	59	4991	<0.0001
ACS-DE/best/1/exp vs ACS-PSO	4855	195	<0.0001
ACS-DE/current-to-best/1 vs ACS-DE/current-to-best/1/bin	4015	1035	<0.0001
ACS-DE/current-to-best/1 vs ACS-DE/current-to-best/1/exp	4361	689	<0.0001
ACS-DE/current-to-best/1 vs ACS-GA	5050	0	<0.0001
ACS-DE/current-to-best/1 vs **ACS-IDE**	77	4973	<0.0001
ACS-DE/current-to-best/1 vs ACS-PSO	5039	11	<0.0001
ACS-DE/current-to-best/1/bin vs ACS-DE/current-to-best/1/exp	2617	2433	0.7540
ACS-DE/current-to-best/1/bin vs ACS-GA	5048	2	<0.0001
ACS-DE/current-to-best/1/bin vs **ACS-IDE**	1	5049	<0.0001
ACS-DE/current-to-best/1/bin vs ACS-PSO	4690	360	<0.0001
ACS-DE/current-to-best/1/exp vs ACS-GA	5046	4	<0.0001
ACS-DE/current-to-best/1/exp vs **ACS-IDE**	13	5037	<0.0001
ACS-DE/current-to-best/1/exp vs ACS-PSO	4717	333	<0.0001
ACS-GA vs **ACS-IDE**	0	5050	<0.0001
ACS-GA vs **ACS-PSO**	1728	3322	0.0061
ACS-IDE vs ACS-PSO	5050	0	<0.0001

Table X: Results of the Wilcoxon test over the ITAE values achieved in simulation by the proposed adaptive control strategies.

Test	R_+	R_-	$p - value$
ACS-DE/best/1/bin vs ACS-DE/best/1/exp	3473	1577	0.0011
ACS-DE/best/1/bin vs ACS-DE/current-to-best/1	2969.5	1980.5	0.0846
ACS-DE/best/1/bin vs ACS-DE/current-to-best/1/bin	4304.5	745.5	<0.0001
ACS-DE/best/1/bin vs ACS-DE/current-to-best/1/exp	4655.5	394.5	<0.0001
ACS-DE/best/1/bin vs ACS-GA	5050	0	<0.0001
ACS-DE/best/1/bin vs **ACS-IDE**	124	4926	<0.0001
ACS-DE/best/1/bin vs ACS-PSO	5047	3	<0.0001
ACS-DE/best/1/exp vs ACS-DE/current-to-best/1	1980.5	3069.5	0.06142
ACS-DE/best/1/exp vs ACS-DE/current-to-best/1/bin	3361	1689	0.0037
ACS-DE/best/1/exp vs ACS-DE/current-to-best/1/exp	3535.5	1514.5	0.0005
ACS-DE/best/1/exp vs ACS-GA	5022	28	<0.0001
ACS-DE/best/1/exp vs **ACS-IDE**	96	4954	<0.0001
ACS-DE/best/1/exp vs ACS-PSO	4619	431	<0.0001
ACS-DE/current-to-best/1 vs ACS-DE/current-to-best/1/bin	4107	943	<0.0001
ACS-DE/current-to-best/1 vs ACS-DE/current-to-best/1/exp	4620	430	<0.0001
ACS-DE/current-to-best/1 vs ACS-GA	5050	0	<0.0001
ACS-DE/current-to-best/1 vs **ACS-IDE**	133	4917	<0.0001
ACS-DE/current-to-best/1 vs ACS-PSO	5030	20	<0.0001
ACS-DE/current-to-best/1/bin vs ACS-DE/current-to-best/1/exp	2494	2556	0.9164
ACS-DE/current-to-best/1/bin vs ACS-GA	4802.5	247.5	<0.0001
ACS-DE/current-to-best/1/bin vs **ACS-IDE**	21	5029	<0.0001
ACS-DE/current-to-best/1/bin vs ACS-PSO	4291	759	<0.0001
ACS-DE/current-to-best/1/exp vs ACS-GA	4865	185	<0.0001
ACS-DE/current-to-best/1/exp vs **ACS-IDE**	33	5017	<0.0001
ACS-DE/current-to-best/1/exp vs ACS-PSO	4429	621	<0.0001
ACS-GA vs **ACS-IDE**	0	5050	<0.0001
ACS-GA vs ACS-PSO	2215	2835	0.2886
ACS-IDE vs ACS-PSO	5050	0	<0.0001

Table XI: Overall wins of the Wilcoxon test for the proposed adaptive control strategies in simulation.

Adaptive control strategy alternative	ISE	IAE	ITAE	Total
ACS-DE/best/1/bin	5	5	5	15
ACS-DE/best/1/exp	4	4	4	12
ACS-DE/current-to-best/1	5	5	4	14
ACS-DE/current-to-best/1/bin	1	2	2	5
ACS-DE/current-to-best/1/exp	1	2	2	5
ACS-IDE	**7**	**7**	**7**	**21**
ACS-GA	1	0	0	1
ACS-PSO	0	1	0	1

Table XII: Parameter bounds.

Variable	*min*	*max*
$\bar{\theta}_0$	0.1	5.0
$\bar{\theta}_1$	1.0×10^{-2}	5.0×10^{-2}
$\bar{\theta}_2$	1.0×10^{-4}	5.0×10^{-4}

Table XIII: Other control performance measurements.

Measurement	ACS-IDE	PI	MRAC	GPIRC
RT_{min}	**0.035**	0.060	1.500	0.075
RT_{max}	**0.050**	0.060	1.585	0.080
$\overline{RT}$	**0.036**	0.060	1.537	0.075
OS_{min}	3.224	8.600	**0.393**	8.553
OS_{max}	8.232	9.442	**0.693**	10.297
$\overline{OS}$	5.896	9.108	**0.495**	9.597
ST_{min}	**0.300**	0.310	2.705	0.465
ST_{max}	0.440	**0.325**	2.805	0.495
$\overline{ST}$	0.353	**0.316**	2.757	0.482
SSE_{min}	**0.105**	0.130	0.154	0.133
SSE_{max}	**0.142**	0.148	0.171	0.158
$\overline{SSE}$	**0.124**	0.136	0.161	0.145

Table XIV: ISE values for the experimental tests of the proposed control strategy based on the IDE, the PI controller, the MRAC and the GPIRC.

Control system alternative	ISE_{best}	ISE_{worst}	$\overline{ISE}$	$std(ISE)$
ACS-IDE	**0.198**	**0.275**	**0.244**	**0.023**
PI	0.349	0.500	0.420	0.045
MRAC	0.231	0.360	0.296	0.035
GPIRC	0.400	0.736	0.540	0.093

Table XV: IAE values for the experimental tests of the proposed control strategy based on the IDE, the PI controller, the MRAC and the GPIRC.

Control system alternative	IAE_{best}	IAE_{worst}	$\overline{IAE}$	$std(IAE)$
ACS-IDE	**0.760**	**0.949**	**0.833**	0.050
PI	1.012	1.185	1.071	0.037
MRAC	0.821	0.971	0.875	**0.036**
GPIRC	1.013	1.249	1.127	0.063

Table XVI: ITAE values for the experimental tests of the proposed control strategy based on the IDE, the PI controller, the MRAC and the GPIRC.

Control system alternative	$ITAE_{best}$	$ITAE_{worst}$	$\overline{ITAE}$	$std(ITAE)$
ACS-IDE	**4.644**	5.986	**5.216**	0.323
PI	6.131	7.177	6.508	0.245
MRAC	5.177	**5.976**	5.441	**0.202**
GPIRC	6.144	7.275	6.689	0.357

Table XVII: Results of the Wilcoxon test over the ISE values achieved in experimentation by the proposed control strategy based on the IDE, the PI controller, the MRAC and the GPIRC.

Test	R_+	R_-	$p - value$
MRAC vs PI	325	0	<0.0001
MRAC vs **ACS-IDE**	4	321	<0.0001
MRAC vs GPIRC	325	0	<0.0001
PI vs **ACS-IDE**	0	325	<0.0001
PI vs GPIRC	314	11	<0.0001
ACS-IDE vs GPIRC	325	0	<0.0001

Table XVIII: Results of the Wilcoxon test over the IAE values achieved in experimentation by the proposed control strategy based on the IDE, the PI controller, the MRAC and the GPIRC.

Test	R_+	R_-	$p - value$
MRAC vs PI	325	0	<0.0001
MRAC vs **ACS-IDE**	58	267	0.0037
MRAC vs GPIRC	325	0	<0.0001
PI vs **ACS-IDE**	0	325	<0.0001
PI vs GPIRC	289	36	0.0002
ACS-IDE vs GPIRC	325	0	<0.0001

Table XIX: Results of the Wilcoxon test over the ITAE values achieved in experimentation by the proposed control strategy based on the IDE, the PI controller, the MRAC and the GPIRC.

Test	R_+	R_-	$p-value$
MRAC vs PI	325	0	<0.0001
MRAC vs **ACS-IDE**	60	265	0.0046
MRAC vs GPIRC	325	0	<0.0001
PI vs **ACS-IDE**	0	325	<0.0001
PI vs GPIRC	255	70	0.0114
ACS-IDE vs GPIRC	325	0	<0.0001

Table XX: Overall wins of the Wilcoxon test for the proposed control strategy based on the IDE, the PI controller, the MRAC and the GPIRC in experimentation.

Control system alternative	ISE	IAE	ITAE	Total
ACS-IDE	**3**	**3**	**3**	**9**
PI	1	1	1	3
MRAC	2	2	2	6
GPIRC	0	0	0	0